ELSEVIER

Journal of Volcanology and Geothermal Research 79 (1997) 223–251

Journal of volcanology and geothermal research

Geochemistry of water and gas discharges from the Mt. Amiata silicic complex and surrounding areas (central Italy)

A. Minissale [a,*], G. Magro [b], O. Vaselli [c], C. Verrucchi [c], I. Perticone [d]

[a] *C.N.R., Centro di Studio per la Minerogenesi e la Geochimica Applicata, Via G. La Pira 4, 50121 Firenze, Italy*
[b] *C.N.R., Istituto di Geocronologia e Geochimica Isotopica, Via Cardinal Maffi 36, 56100 Pisa, Italy*
[c] *Dipartimento di Scienze della Terra, Via G. La Pira 4, 50121 Firenze, Italy*
[d] *ENEL, Vice Direzione Attivita' Geotermiche, Via A. Pisano 120, 56100 Pisa, Italy*

Received 21 August 1996; accepted 10 June 1997

Abstract

The Mt. Amiata volcano in central Italy is intimately related to the post-orogenic magmatic activity which started in Pliocene times. Major, trace elements, and isotopic composition of thermal and cold spring waters and gas manifestations indicate the occurrence of three main reservoir of the thermal and cold waters in the Mt. Amiata region. The deepest one is located in an extensive carbonate reservoir buried by thick sequences of low-permeability allochthonous and neo-autochthonous formations. Thermal spring waters discharging from this aquifer have a neutral Ca-SO_4 composition due to the presence of anhydrite layers at the base of the carbonate series and, possibly, to absorption of deep-derived H_2S with subsequent oxidation to SO_4^{2-} in a system where pH is buffered by the calcite–anhydrite pair (Marini and Chiodini, 1994). Isotopic signature of these springs and N_2-rich composition of associated gas phases suggest a clear local meteoric origin of the feeding waters, and atmospheric O_2 may be responsible for the oxidation of H_2S. The two shallower aquifers have different chemical features. One is Ca-HCO_3 in composition and located in several sedimentary formations above the Mesozoic carbonates. The other one has a Na-Cl composition and is hosted in marine sediments filling many post-orogenic NW–SE-trending basins. Strontium, Ba, F, and Br contents have been used to group waters associated with each aquifer. Although circulating to some extent in the same carbonate reservoir, the deep geothermal fluids at Latera and Mt. Amiata and thermal springs discharging from their outcropping areas have different composition: Na-Cl and Ca-SO_4 type, respectively. Considering the high permeability of the reservoir rock, the meteoric origin of thermal springs and the two different composition of the thermal waters, self-sealed barriers must be present at the boundaries of the geothermal systems. The complex hydrology of the reservoir rocks greatly affects the reliability of geothermometers in liquid phase, which understimate the real temperatures of the discovered geothermal fields. More reliable temperatures are envisaged by using gas composition-based geothermometers. Bulk composition of the 67 gas samples studied seems to be the result of a continuous mixing between a N_2-rich component of meteoric origin related to the Ca-SO_4 aquifer and a deep CO_2-rich component rising largely along the boundaries of the geothermal systems. Nitrogen-rich gas samples have nearly

* Corresponding author. Fax: +39-55-284571; e-mail: minissa@mailserver.idg.fi.cnr.it.

0377-0273/97/$17.00 © 1997 Elsevier Science B.V. All rights reserved.
PII S0377-0273(97)00028-0

atmospheric N_2/Ar (= 83) and $^{15}N/^{14}N$ ($\delta = 0‰$) ratios whereas CO_2-rich samples show anomalously high $\delta^{15}N$ values (up to +6.13 ‰), likely related to N_2 from metamorphic schists lying below the carbonate formations. On the basis of average $^{13}C/^{12}C$ isotopic ratio ($\delta^{13}C$ around 0‰), CO_2 seems to originate mainly from thermometamorphic reactions in the carbonate reservoir and/or in carbonate layers embedded in the underlying metamorphic basement. Distribution of $^3He/^4He$ isotopic ratios indicates a radiogenic origin of helium in a tectonic environment that, in spite of the presence of many post-orogenic basins and mantle-derived magmatics, can presently be considered in a compressive phase. © 1997 Elsevier Science B.V.

Keywords: geochemistry; water; gas; stable isotope; geothermics; Mt. Amiata; Central Italy

1. Introduction

Post-orogenic magmatic activity occurred in the northern Apennines (central Italy) during Pliocene to Quaternary times and produced hybrid (crustal anatectic—upper mantle; Poli et al., 1984; Giraud et al., 1986; Peccerillo et al., 1987), anatectic (Barberi et al., 1971) and subcrustal primary K-rich silica-undersaturated magmas in Tuscany and Lazio, respectively (Peccerillo et al., 1987). These magmatic activities are associated with geothermal anomalies which may have persisted for relatively long periods (2–3 Myr; Calore et al., 1981) and been generally more widespread than the volcanic areas on surface. This is particularly evident at Larderello (the most important geothermal field in Italy), where volcanic outcrops are only found 25 km away from the geothermal field itself, and drill holes have encountered only small 3.8 Ma microgranitic dikes at > 3000 m depth (Villa et al., 1987).

Deep geothermal wells in the peri-Tyrrhenian belt show relatively uniform temperatures of 300–400°C at depths of 3–4 km (CEE, 1988). At greater depths, high heat flow is due to deep-seated (6 to 10 km) masses close to their melting point (Puxeddu, 1984). Heat is transferred to shallow depth by conduction and by convection in a regional aquifer hosted in Mesozoic limestone formations ('Tuscan' series), sometimes piled up in accretional prism (Pandeli et al., 1991). This aquifer plays an important role in increasing shallow thermal gradients, so that in those areas, where the aquifer is confined and self-sealed (Travale, Mt. Amiata, Latera and Bolsena, Fig. 1), reservoirs at > 200°C form at < 1 km depth (Carella et al., 1985).

At the margins of such geothermal fields, a large number of $Ca\text{-}SO_4$ thermal springs, generally associated with gas emissions, are found, that may indicate the widespread convective thermal anomaly. Lotti (1910) interpreted these thermal springs as the result of a low-temperature hydrothermal residual activity related to the final stages of the Apenninic post-orogenic magmatism. Trevisan (1951), Tonani (1957) and Bencini et al. (1977) suggested that the thermal $Ca\text{-}SO_4$ character of these waters could imply the exothermic hydration process of anhydrite strata ('Burano formation') which occur at the base of the Mesozoic limestones. Deep drill holes, at both Larderello, Travale and Mt. Amiata (Batini et al., 1995) and in some Pb–Cu–Zn mining areas in southern Tuscany (Vighi, 1958, 1966) indicate the occurrence of gypsum where temperature at depth is < 150°C.

More recently, Baldi et al. (1973), Ceccarelli et al. (1987a), Minissale and Duchi (1988) suggested that the central Italy geothermal anomaly is mostly related to a deep circulation of meteoric waters in an area of high regional heat-flow (Calamai et al., 1976b). This circulation occurs primarily in a thick (up to 3.5 km; Buonasorte et al., 1991) sequence of carbonate rocks which also host high salinity geothermal systems. However, interaction between the geothermal fluids and the thermal spring waters may be restricted by self-sealing processes (Facca and Tonani, 1967).

Thermal spring waters discharging in the areas of limestone outcrops in central Italy (Duchi et al., 1985, 1987a,b, 1992; Chiodini et al., 1991; Celati et al., 1991) show the following chemical and isotopic features:

(1) constant flow rate and chemical and isotopic composition;

(2) $^{18}O/^{16}O$ and D/H isotopic ratios suggesting a meteoric origin;

(3) low tritium values suggesting a relatively long residence time underground (> 40 years).

As mentioned before, most of the thermal springs have a Ca-SO_4 composition although a limited number of saline Na-Cl springs are also present. The latter have been interpreted as due to either mixing between Ca-SO_4 thermal waters and descending cold fossil seawater trapped in the Neogene sediments (Francalanci, 1959; Duchi et al., 1992) or to water circulation in the Paleozoic basement (Panichi et al., 1974; Panichi, 1982). The latter, although lying below the Mesozoic limestones, may occur adjacent to the limestones in areas of folded terraines. Since occurrence of saline Na-Cl type fluids is closely related to the geothermal systems in central Italy at Larderello (Panichi et al., 1974), Mt. Amiata (Scandiffio, pers. commun.), Latera (Gianelli and Scandiffio, 1989), Torre Alfina (Buonasorte et al., 1988) and Cesano (Calamai et al., 1976a), leakage of these fluids into the regional Ca-SO_4 acquifer cannot be ruled out.

Continental margins are characterised by high CO_2 emissions (Barnes et al., 1978, 1984) and CO_2 vents are very common in central Italy (Duchi and Minissale, 1995). Their origin has been related to either hydrolysis of limestone in the Mesozoic formations (Kissin and Pakhomov, 1967) or to thermometamorphic processes in the Paleozoic basement (Gianelli, 1985; Duchi et al., 1992). Regardless the origin, rising CO_2 may strongly affect the chemical composition of the aquifers through ion exchange processes as well as calcite and/or gypsum precipitation in response to P_{CO_2} variations (Marini and Chiodini, 1994). The precipitation is likely to occur at the margins of the geothermal fields where thermal conditions may change dramatically in short distances (Cavarretta et al., 1985).

This paper presents some published data and a large set of unpublished (by courtesy of ENEL Italian Electricity Agency) chemical and isotopic data on thermal and cold waters and associated gases obtained in four prospecting campaigns in central Italy (Ceccarelli et al., 1987b, 1988, 1989, 1991), as well as data for deep fluids from the Travale–Mt. Amiata–Latera geothermal areas. The main goals of this study are:

(1) to assess the origin of waters which supply both the springs and the deep geothermal fluids;

(2) to assess the origin of the gas components and discuss their interaction with shallow aquifers;

(3) to evaluate the trace element distribution in waters and their usefulness in the reconstruction of circulation paths;

(4) to correlate the chemical and isotopic data of thermal waters and gases with recent neotectonic studies;

(5) to delineate as yet undiscoverd areas of high-enthalpy waters.

2. Geological setting of the Travale, Mt. Amiata and Latera geothermal fields

The area under study is morphologically characterised by the Mt. Cetona ridge (1078 m a.s.l.), the Mt. Amiata (1770 m a.s.l.) linear silicic complex (Ferrari et al., 1996), the Bolsena caldera and the Quaternary K-rich and high-*K* volcanics of Vulsini Mts. and Cimini Mts. (Fig. 1). The Mt. Amiata, Vulsini Mts. and Cimini Mts. volcanic products, characterized by high permeabitily in the lavas and very low permeability in the pyroclastics, are underlain by sedimentary and metamorphic units with the following sequence from the bottom to the top: (1) low-to-medium permeability Paleozoic metamorphic basement; (2) high-permeability Mesozoic limestone formations ('Tuscanids'); (3) low-permeability allochthonous flysch formations ('Ligurids'); and (4) low-permeability Mio-Quaternary continental and marine post-orogenic sediments (Abbate et al., 1970). The Mesozoic limestones are the main reservoir for the production of the geothermal fluids, whereas the overlying tectonic units act as an impermeable caprock. This area has also been affected by NW–SE-oriented tensive tectonics which caused the formation of many Neogene basins (e.g. the Siena and Radicofani basins in Fig. 1) whose sediments have been uplifted to 1000 m a.s.l. in the surrounding areas of Mt. Amiata (Sestini, 1932). Gianelli et al. (1988) interpreted this uprising as the result of the emplacement of a large intrusive granite body at a relatively shallow level in the crust (5–6 km).

The Travale geothermal field is situated at 15 km east of the Larderello field (Fig. 1) and electrical power plants producing a total of 90 MW have been installed there. It is a steam-dominated system with maximum temperature of production of 270°C. The

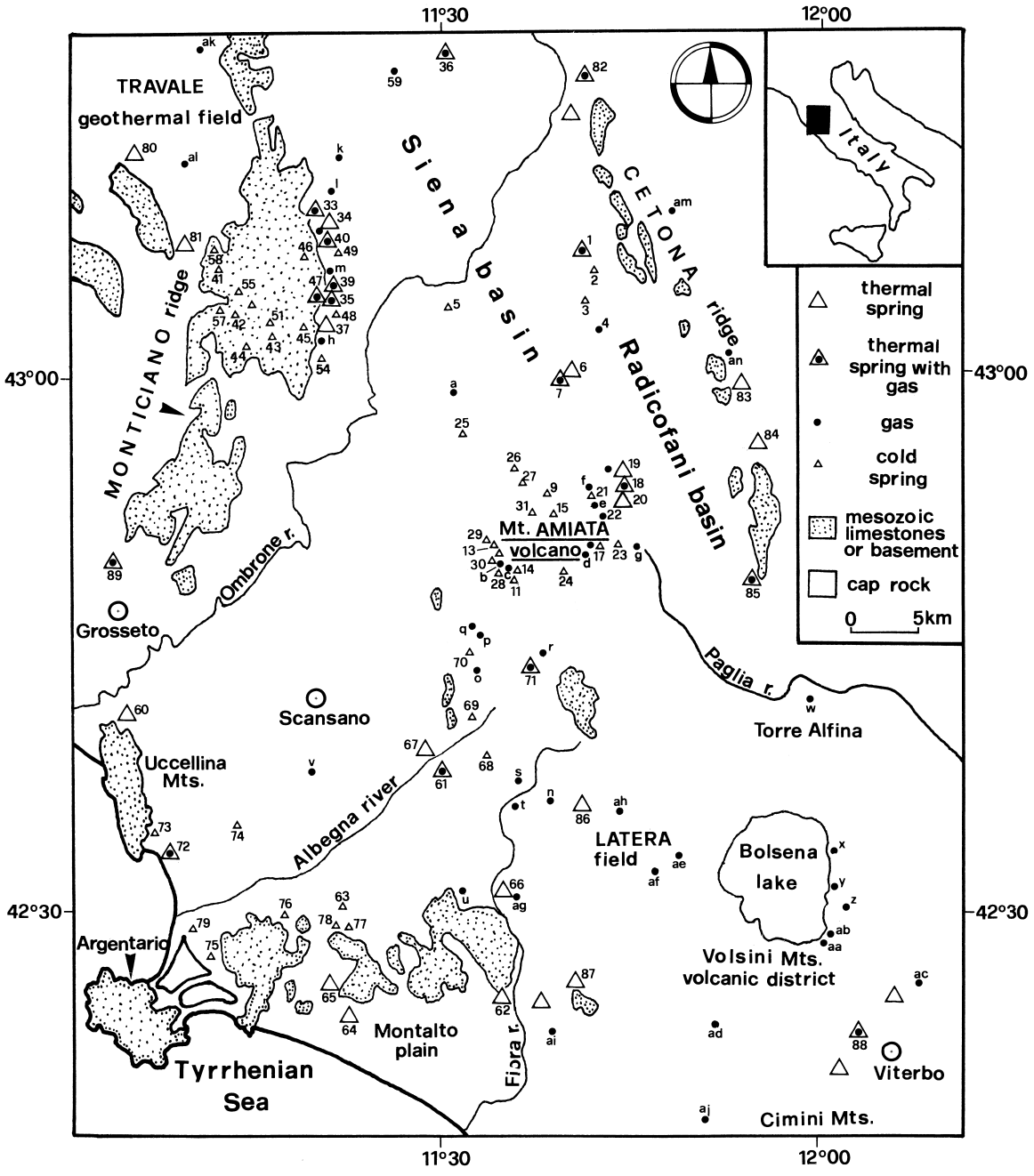

Fig. 1. Sketch map of the study area with locations of the water and gas sampling points. Sites without numbers refer to manifestations not sampled in this study.

geothermal reservoir is located in both the Mesozoic carbonatic horizon and the Paleozoic metamorphic basement at 600–1500 m depth (Barelli et al., 1995).

The Mt. Amiata geothermal area locates at 60 km southeast of Travale. The two Bagnore and Piancastagnaio fields produce a two-phase fluid origi-

nating from two separate horizons of production. The shallower is at 500–1000 m depth in the carbonates and produces a 200–230°C fluid whereas the deeper one (> 3000 m) is in the Paleozoic basement where temperature ranges from 300 to 350°C (Calamai et al., 1970; Gianelli et al., 1988).

Moving to the south, the Latera geothermal field produces a few megawatts from a liquid-dominated reservoir (800–1000 m deep) containing Na-Cl water at 200–230°C (Bertrami et al., 1984). Wells at Torre Alfina (600–1000 m deep) have encountered a liquid-dominated system with Na-Cl waters at 150°C (Cataldi and Rendina, 1973; Buonasorte et al., 1988). There, the low reservoir temperatures limit the productive extraction of the geothermal energy.

3. Analytical methods

Seventy-nine water samples (24 thermal, 51 cold and 4 stream waters), 8 samples from the Mt. Amiata geothermal wells and 67 surface gas samples have been analysed for major, trace and isotopic composition. Temperature, electrical conductivity, pH, Eh, Rn concentration and flow rate have been measured in the field. Isotopic composition of oxygen and hydrogen in water and $^{13}C/^{12}C$ in CO_2, $^{15}N/^{14}N$ in N_2, $^{40}Ar/^{36}Ar$ and $^{3}He/^{4}He$ ratios have been measured in selected thermal waters and gases.

In order to determine heavy metals, water samples were treated in the field as follows: (1) filtered with 45 μm filter; (2) acified with HNO_3; and (3) diluted (1:10) for silica determination. Analytical methods are as follows; HCO_3 by titration with HCl; SiO_2 by colorimetry; Ca, Mg, Sr and Fe by atomic absorption spectrophotometry (AAS); Na, K, Li, Rb and Cs by emission spectrophotometry; Cl, SO_4, I and Br by ion chromatography; B, As, Sb, Ba, Zn and $Al_{(tot)}$ by graphite furnace AAS; NH_4 and F by potentiometry.

Gas samples were collected in two pre-evacuated 100 cm^3 bottles, one of which contains 50 ml of 4M NaOH to concentrate the non reactive components (Giggenbach, 1975). CO_2, N_2, H_2S and $O_2 + Ar$ were determined by gaschromatography using a thermal conductivity detector, while H_2, CO, CH_4 and C_2H_6 were analyzed with a He ioniser detector. He contents were determined with a Du Pont 120-SSA spectrometer; He/Ne and $^{40}Ar/^{36}Ar$ ratios were measured with a quadrupole Spectralab 200 VG-Micromass spectrometer; $^{3}He/^{4}He$ ratio was measured with a magnetic MAP 215-50 mass spectrometer. Some of the $^{13}C/^{12}C$ in CO_2 and all the $^{15}N/^{14}N$ isotopic ratios (Minissale et al., 1995) were determined with a Finnigan MAT 251 spectrometer.

4. Chemical composition

4.1. Major elements in waters

Results are listed in Tables 1–5 and the classification of water samples according to the Langelier and Ludwig (1942) diagram is shown in Fig. 2.

Most of thermal spring waters are in the Ca-SO_4 field with the exception of four samples in the Siena basin (#33, #35, #36, #47) and sample #72 located along the Tyrrhenian shoreline that plot in the Na-Cl sector. The saline geothermal fluids from the Latera and Mt. Amiata wells also lie in the Na-Cl sector (Fig. 2). Owing to the low solubility of Ca-SO_4 and Mg co-precipitation in clay minerals at high temperature (Ellis, 1971), these geothermal fluid samples fall along the (Ca + Mg) = 0 axis, but they have a higher HCO_3 content with respect to seawater (sw).

Although plots of cold water samples scatter all over the Langelier–Ludwig diagram, most of them have a groundwater Ca-HCO_3 composition. Low-pH samples are SO_4-rich waters, which is likely due to the oxidation of H_2S to SO_4 in subaerial environment, and are indicated as 'acidic waters' (Fig. 2). These waters plot along the $HCO_3 = 0$ axis since at pH < 4.3 the bicarbonate ion is completely transformed into CO_2. A few cold springs have a Na-Cl composition. They emerge in the outcrop areas of the Neogene formations and are likely related to fossil seawater trapped inside the sediments (Duchi et al., 1992).

Most of the samples could be interpreted as a mixture of the following three endmembers: (1) seawater (or fossil seawater); (2) Ca-HCO_3 groundwater; and (3) Ca-SO_4 thermal water. The so-called 'CO_2-interaction' lines are others possible evolutionary paths for waters with any original composition because CO_2 is extremely ubiquitous at shallow level in the crust in central Italy (Panichi and Tongiorgi, 1976). High CO_2 concentration causes ionic

Table 1
Main components of cold, shallow and stream samples in the study area

No.	Name	Type	Elev.	Flow	*t*	Cond.	pH	Eh	TDS	Ca	Mg	Na	K	HCO_3	Cl	SO_4	B	SiO_2
2	S.Anna in Camprena	s	396	0.3	12.0	805	7.69	393	721	136	27.3	9.0	1	508	16.8	17	0.29	7.3
3	Molino del Bagnolo	s	300	0.03	17.0	1538	6.58	195	1672	266	84.4	68.7	6.9	685	69.9	488	2.1	13
4	Acqua Puzzola	gp	340	0.01	11.0	5820	2.05	713	6140	581	143.0	97.7	15.2	0	73.8	4680	0.68	109
5	Fonte Petri	sg	160	0.03	19.5	9780	8.4	−185	7713	13	21	2790	21.5	1787	2765	258	15.8	8.8
8	Acqua Rossa	s	835	2.2	12.0	1070	6.27	160	1327	310	10.7	16.0	1.1	970	11	1.5	0.48	12.3
9	Tre Fonti	s	740	0.8	14.0	540	7.11	187	582	72.9	35.6	20.6	1.4	410	10.5	26.8	0.45	9.9
10	Acque Calde	s	975	0.5	18.0	139	7.02	283	146	16	5.2	10.2	4.2	75.7	9.6	6.7	0.62	70.9
11	Polla di Sotto	s	775	0.6	19.0	297	5.86	327	275	21.4	5.4	18.7	13.8	32.9	25.8	46.6	3.1	80.1
12	Bagnoli	s	695	3.0	21.0	134	6.84	203	158	9.9	4	4.5	4.2	39.1	7.3	20.7	0.84	69.2
13	Triaco	s	650	0.05	17.0	118	6.5	361	157	9.3	2.8	8.8	5.2	45.2	8.4	6.5	0.51	68.9
14	Acqua Forte Bagnore	w	800	nd	18.0	1449	6.13	235	1911	411	37.1	9.7	4.4	1263	42.4	152	0.64	16.4
15	Acqua Gialla	s	1050	0.5	8.0	60	6.15	209	118	6.2	1.4	6.1	4	38.4	6.8	2.3	0.34	51.7
16	Acqua Passante 1	s	1052	0.03	11.0	141	4.15	643	167	5.4	1.3	4.6	5	0	5	80	0.2	54.6
17	Acqua Passante 2	s	1050	0.06	12.0	495	6.15	−45	904	215	7.5	4.3	3.1	536	5.6	114	0.13	30
21	Galleria Casanova	sg	584	7.0	18.5	1760	6.08	11	2516	593	58.7	8.1	1.6	1320	10.4	559	0.17	10.2
22	Putizza Rondinaia	gp	660	0.01	18.0	540	4.18	81	599	98.1	13.3	7.1	2	0	7.8	396	0.45	36.9
23	Galleria Nuova Italia	sg	780	25.0	16.0	790	4.45	506	937	167	19.8	10.2	9.6	0	6.1	634	0.3	52
24	Tre Case	s	805	0.1	23.0	324	7.53	333	324	37.2	18.1	16.8	0.97	200	9.2	11.7	0.19	20.5
25	Acqua Salata	s	240	nd	20.0	5250	7.02	253	5342	77.2	69.9	1322	25.7	2592	305	768	90.4	24.5
26	Pian delle Borrelle	s	515	0.3	15.0	583	7.55	336	646	125	15.7	15.6	0.16	435	17	22.7	1	8.2
27	La Tagliata	s	670	0.6	13.0	422	6.97	321	476	106	9.6	9.4	0.47	323	6.8	13.1	0.2	6.7
28	La Vena	s	730	4.5	15.0	113	6.78	267	150	8.6	2.5	7.8	4.6	44.5	8.6	10	1.4	60.7
29	Il Pino	s	630	10.0	15.5	130	6.75	303	166	11	3.5	9.4	4.8	45.1	9.9	7.2	0.76	65.2
30	Acqua Forte Ontani	s	830	0.1	12.0	33	5.63	393	28	1.6	1	3.8	0.25	6.1	4.8	2.5	0.37	6.3
31	Capo Vetra	s	1085	nd	8.0	59	6.45	366	86	6.1	1	4.5	2.6	20.7	8	1.4	0.38	35.9
32	Pozzo Hotel Aiole	w	830	nd	17.0	344	5.95	331	306	33	9.3	18.6	12	52.5	20.4	69	0.4	59.3

41	Podere Fogarone	s	570	0.15	15.0	515	7.6	1	544	115	7.9	9.8	1.5	360	19.3	19.8	0.1	10.6
42	Solforica Riguardello	s	370	0.01	15.0	1161	6.5	34	1319	262	63.4	10.9	1.4	378.2	15.3	566	0.1	14.2
43	Fontaccia	s	355	1.5	15.0	602	6.6	294	663	152	5	10.5	0.8	451.4	20.3	16	0.1	6.3
44	Acquanera	s	475	0.25	20.0	338	7.0	384	330	55.8	14.3	10.7	0.4	207.4	15.2	10.8	0.3	15.1
45	Acqua Bolle S.Antonio	sg	300	0.01	16.0	1802	6.28	332	2425	434	84.8	54.3	3	1800	36.8	< 0.2	0.7	9.2
46	La Pigna	s	320	1.25	14.0	451	7.36	374	484	112	4.1	5.9	0.4	335.5	11.2	10	0.1	5.3
48	Acqua Frizzante	s	170	0.05	16.0	2290	6.2	49	2294	480	71.1	13.5	1.1	1677.5	21.6	14.2	0.8	10.3
49	Acqua Puzzola Funina	s	160	1.5	20.0	3140	5.9	− 106	3227	668	132	43.9	5.7	951.6	51.1	1350	11.5	18
50	Fosso Belagaio	s	440	0.01	16.0	265	3.55	164	160	9.1	6.5	7.6	1.9	0	13.7	87.2	0.3	13.3
51	Fosso Arlecchino	s	385	0.2	18.0	571	6.7	344	533	81.4	13	17.7	1.1	366	28.6	16.8	0.2	7.8
53	Acqua Rossa	s	360	0.01	21.0	705	8.2	134	507	63.8	40.9	20.3	0.6	213.5	29.2	134	< 0.1	6.2
54	Badia Ardenghesca	s	160	1.0	18.0	1346	6.7	334	1103	215	48.1	30.6	1.4	366	51.9	376	0.4	9
55	Fiume Farma 1	r	325	nd	15.0	937	7.53	434	831	161	25.1	9.5	0.9	207.4	18	300	0.1	7.4
56	Fiume Farma 2	r	nd	nd	17.0	1622	7.22	204	1250	210	42.9	86.7	12	299	124	430	29.7	11.3
57	Fiume Bardellone	r	335	nd	16.0	1035	7.75	275	814	178	30.2	9.2	1.1	195	14.2	376	0.2	7.4
58	Fiume Merse	r	nd	nd	18.0	1791	7.11	322	1623	362	64.7	9.8	1.6	378	11.4	780	1.5	9.1
59	Case Ropole	sg	190	1.2	16.0	30250	6.37	71	23401	304	622	6760	120	6100	8850	354	185	14.6
63	Le Croste	s	168	0.35	18.0	516	7.05	324	553	117	8.8	28.4	1.2	289.8	39.4	54.8	0.4	12.2
68	Fonte delle Piane	s	350	0.06	20.0	686	7.08	298	779	116	42	31.1	1.4	472.3	51	51.3	0.31	12.3
69	Fontacce	s	525	0.2	14.0	409	7.16	349	502	117	3.3	12.7	0.7	280.7	21.2	56.4	< 0.1	8.5
70	Campo delle Pozze	s	650	0.01	15.0	1470	8.82	284	1776	5.8	3.2	556	1.7	982.4	62.2	129	10.2	10.9
73	Podere S.Giuseppe	w	6	nd	20.0	2290	6.84	204	1891	233	52.8	314	28.2	353.3	593	296	2.6	12.3
74	Vergheria	s	44	1.0	18.0	877	6.72	315	871	178	22.3	57.9	2.7	400.3	134	55.4	0.3	18.8
75	Pozzo irriguo 2	w	30	nd	19.0	712	6.9	nd	696	137	19.2	41.1	3.3	362.4	72	42	0.3	17.5
76	Lago Scuro	l	7	nd	20.0	1410	8.93	nd	1318	152	68.8	158	30.7	99.5	262	519	23.9	< 0.3
77	Lago Acquato	l	110	nd	14.0	1060	7.88	nd	1097	126	38	161	2.1	279.5	215	224	0.33	49.1
78	Lago Cerro Sughero	l	95	nd	17.0	847	7.9	nd	762	103	28.2	100	3.8	245.9	220	56.3	0.24	2.4
79	Pozzo Campolungo	w	5	nd	18.0	1560	6.94	nd	1366	182	62.1	178	4	350.8	476	85.6	1	23.3

Elevation (elev.) in m; flow rate (flow) in l/s; temperature (t) in °C; conductivity (cond.) in μS/cm; Total dissolved solids (TDS), Ca, Mg, Na, K, HCO_3, Cl, SO_4, B and SiO_2 in mg/kg.
s = spring; sg = spring with associated gas; w = well; gp = stagnant water associated with gas; r = river; l = lake.
nd = not determined.

Table 2
Main components in thermal springs emerging from the carbonate reservoir

No.	Name	Type	Elev.	Flow	t	Cond.	pH	Eh	TDS	Ca	Mg	Na	K	HCO_3	Cl	SO_4	B	SiO_2
1	Bagnaccio S.G.Asso	tsg	303	10.0	29.5	2700	6.03	306	3913	760	188	58.3	11.4	1253	59.2	1570	6.5	21.7
6	Cava Solet	ts	290	2.0	48.0	4560	6.87	295	3853	730	207	71.1	16.5	1049	60	1695	6.7	29.3
7	Bagno Vignoni	tsg	306	nd	41.0	3960	6.77	303	3913	722	208	73.6	18.3	1014	63.1	1760	7	29.81
8	Bagni S.Filippo	tsg	603	0.3	51.0	3640	6.43	−111	4317	859	193	24.1	9	1943	14.6	1245	1.6	40.81
9	Passante S.Filippo	tsg	490	0.5	28.5	1950	6.35	337	2305	446	115	17.6	6.4	796	13.2	880	0.9	26.4
20	Fosso bianco	tsg	530	1.0	46.5	nd	6.38	−69	3450	657	176	23.9	7.6	1410	15.4	1180	1.5	39.1
33	Doccio bis	tsg	160	0.15	49.0	7020	5.99	9	4950	685	108	1090	49.1	1165	1490	1340	95	54.2
34	Bagnolo di Montisi	ts	145	4.0	33.0	4860	5.82	61	4542	662	117	532	34.2	866	632	1600	49	31.2
35	Mortaione	ts	150	0.01	36.0	10800	6.22	−6	9159	392	74	2040	320	2208	3140	3.7	810	40.8
36	Acqua Borra	tsg	200	0.8	37.0	16610	6.37	84	14719	640	103	3970	245	3366	4840	1020	375	24.3
37	Caldanelle	ts	197	3.0	37.0	2110	6.23	68	2813	645	109	16.7	1.8	427	22.3	1560	0.4	16.3
38	Molin del Tifo	ts	240	0.75	26.0	1770	7.5	334	2292	544	84	10.4	1.1	214	12.5	1400	0.2	17.1
39	Petriolo	tsg	160	8.0	45.0	2970	6.15	−156	4235	806	145	136	20.2	1403	185	1440	49.6	23.7
40	Macereto	tsg	160	5.0	22.0	1491	6.23	−96	1855	371	66	22.9	3.2	750	30.6	586	5.2	12.2
47	Guado di Pietrafessa	sg	185	0.01	30.0	10580	6.0	154	8779	474	88	1800	256	2440	2830	22.5	724	38.5
52	Podere Pratella	tsg	200	0.01	20.0	3040	6.2	−16	3053	639	123	51.4	5.3	885	51.9	1260	8.8	14.4
60	Alberese	ts	30	nd	29.0	2380	6.09	−116	2549	462	91	168	8.1	781	312	681	15.2	21.9
61	Bagni di Saturnia	tsg	156	400	37.0	3250	6.18	474	3156	599	131	75.1	9.2	641	69.4	1470	94	22.5
62	Pozzo Irriguo	w	150	nd	21.0	1980	6.71	209	2665	475	118	91.1	15.7	787	70.6	987	18.9	13.4
64	Poggio Cavallucciaro	sg	60	0.2	19.0	2380	6.61	−136	2344	503	97	43	3.1	378	73.8	1220	0.6	14
65	Lasco delle Vene	s	90	250	20.0	1600	6.76	284	1699	382	70	24.4	1.6	345	47.2	808	0.4	11.6
66	Scarceta	ts	115	0.01	23.0	2460	6.57	nd	3101	694	139	20.8	1.6	354	30.5	1830	1.3	15
67	Le Caldine	ts	195	2.0	37.0	3240	6.5	34	3125	590	118	81.5	10.2	602	73.6	1470	111	23
71	Galleria Morone	sg	342	28.0	19.0	2150	6.86	−41	3014	701	115	22.7	3.3	830	14.2	1310	0.8	9.6
72	Bagni dell' Osa	tsg	6	56.0	32.0	22800	6.3	−136	18542	1180	476	4800	162	519	8630	2660	35	20.2
80	Bagni Galleraie[a]	ts	340	1.2	32.0	3800	6.31	110	3131	721	88	9	2	769	10	1537	11	19
81	Vene di Ciciano[a]	ts	335	900	22.0	2500	6.73	170	1610	344	67	8.3	1.6	415	5.3	768	1	10.2
82	Rapolano[a]	tsg	290	nd	38.0	4500	6.5	nd	6527	932	230	448	59	3087	348	1325	65	29
83	Chianciano[a]	ts	450	nd	36.0	2330	6.3	nd	3224	600	168	20	5.1	732	19	1680	0.7	28.1
84	Sarteano[a]	ts	560	60.0	24.0	1490	6.7	nd	1783	360	86	7.1	1.8	451	12.8	864	0.1	12.2
85	S.Casciana Bagni[a]	tsg	508	40.0	42.0	2030	6.4	nd	2277	420	96	67	2	427	92	1152	1.1	21
86	Pitigliano[a]	ts	351	6.0	36.0	3800	6.46	nd	2628	530	123	7.8	46.8	397	11.4	1555	0.5	20.1
87	Canino[a]	ts	151	60.0	40.0	6420	6.42	nd	2887	546	100	128.8	29.6	665	74.6	1344	68	43.3
88	Bagnaccio[a]	tsg	310	10.0	65.0	4300	6.4	nd	3115	608	143	35.4	33.2	1031	17.8	1248	6.2	48.8
89	Roselle[a]	tsg	30	50.0	36.0	2340	6.95	200	2714	600	122	29.8	3.7	287	39.1	1632	0.9	31.1

Elevation (elev.) in m; flow rate (flow) in l/s; temperature (t) in °C; conductivity (cond.) in μS/cm; Total dissolved solids (TDS), Ca, Mg, Na, K, HCO_3, Cl, SO_4, B and SiO_2 in mg/kg.
s = spring; sg = spring with associated gas; ts = thermal spring; tsg = thermal spring with associated gas; w = well.
nd = not determined.
[a]Original data in Minissale and Duchi (1988).

exchange of Ca ions in the solutions with Na (K) ions contained in clay mineral lattice. Since clay minerals are abundant in both the 'Ligurids' and the post-orogenic clastic formations, addition of CO_2 may modify the chemical compositions of waters in confined aquifers to a Na-HCO_3 chemical composition (Drever, 1982).

4.2. Trace elements in water samples

Abundances of Cs, Rb, As, I, Sb and Zn, in both cold and thermal spring waters (Tables 3 and 4) are low and below their instrumental detection limits in most of samples. $Al_{(tot)}$ and Fe have shown high concentration (up to 44 and 390 ppm, respectively) only in the relatively low-pH waters, indicating that their content is mainly controlled by dissolution of country rocks with acid fluids formed through H_2S oxidation.

In contrast, Sr proved to be positively correlated with emerging temperatures of springs (Fig. 3), and plots of Sr against F (Fig. 4) can be used to delineate

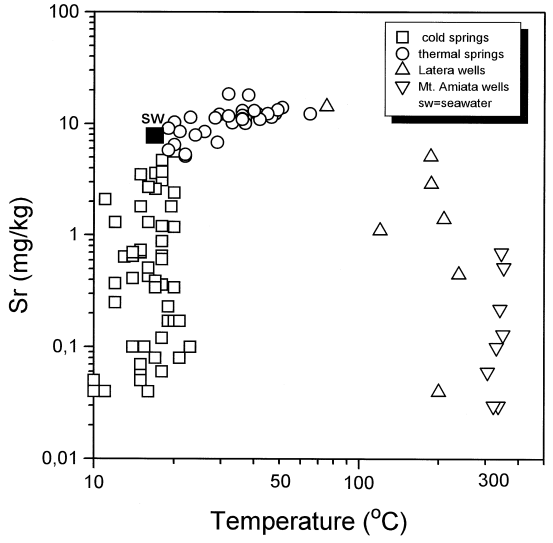

Fig. 3. Strontium vs. emergence temperature (°C) diagram. Temperatures for geothermal wells are measured at the bottom.

springs whose waters circulate through the regional Ca-SO_4 aquifer. The high Sr contents are easily explained in thermal springs, because this element intimately associates with Ca and hence is enriched in the Ca-SO_4 samples. Fluorine concentration may be controlled by equilibration with secondary anhydrite and fluorite inside the Mesozoic carbonates

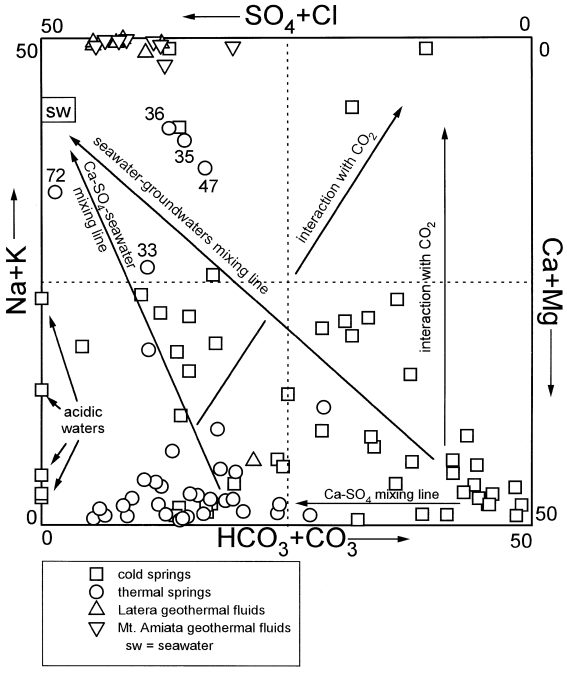

Fig. 2. Langelier and Ludwig (1942) diagram for spring water samples and some geothermal fluids of wells from Latera and Mt. Amiata.

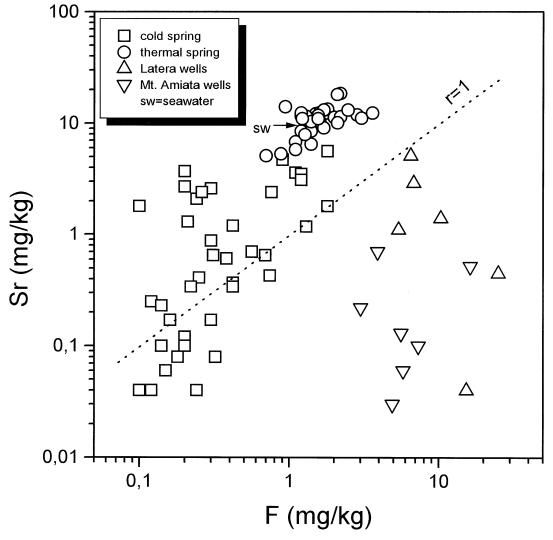

Fig. 4. Strontium vs. F diagram.

Table 3
Minor, trace and isotopic composition of cold, shallow and stream samples

No.	Name	NH_4	Li	F	Rb	Cs	Ba	Sr	Br	I	As	Al(t)	Fe	Sb	Zn	Al(m)	H_2S	$\delta^{18}O$	δD
2	S.Anna in Camprena	< 0.1	< 0.01	0.12	< 0.04	< 0.2	0.09	0.25	< 0.1	< 0.2	< 0.005	0.02	0.08	0.004	0.02	nd	nd	nd	nd
3	Molino del Bagnolo	0.32	0.1	1.1	0.04	< 0.2	0.02	3.6	0.2	< 0.2	< 0.005	< 0.02	1.3	0.004	0.015	nd	nd	nd	nd
4	Acqua Puzzola	< 0.1	0.17	0.24	< 0.04	< 0.2	0.011	2.1	< 0.1	< 0.2	0.019	44.0	390.0	0.006	1.9	nd	nd	nd	nd
5	Fonte Petri	13.2	0.3	1.8	0.04	< 0.2	0.3	1.8	9.3	1.3	0.010	0.02	0.04	0.055	0.006	< 0.02	57.0	nd	nd
8	Acqua Rossa	0.12	0.01	0.21	< 0.04	< 0.2	0.07	1.3	< 0.1	< 0.2	0.005	< 0.02	6.0	0.004	< 0.002	nd	nd	nd	nd
9	Tre Fonti	< 0.1	0.02	0.25	< 0.04	< 0.2	0.07	0.41	< 0.1	< 0.2	< 0.005	< 0.02	0.37	< 0.01	< 0.002	nd	nd	nd	nd
10	Acque Calde	< 0.1	0.04	0.2	< 0.04	< 0.2	0.002	0.12	< 0.1	< 0.2	0.012	0.02	0.02	0.006	< 0.002	nd	nd	nd	nd
11	Polla di Sotto	< 0.1	0.03	0.16	0.12	< 0.2	0.021	0.17	< 0.1	< 0.2	< 0.005	0.03	< 0.01	< 0.01	0.007	< 0.02	nd	nd	nd
12	Bagnoli	< 0.1	0.04	0.32	0.04	< 0.2	0.003	0.08	< 0.1	< 0.2	0.036	0.03	0.97	< 0.01	< 0.002	< 0.02	nd	nd	nd
13	Triaco	0.2	0.02	0.18	< 0.04	< 0.2	< 0.01	0.08	< 0.1	< 0.2	0.020	< 0.02	< 0.01	< 0.01	0.009	nd	nd	nd	nd
14	Acqua Forte Bagnore	0.54	0.04	0.3	< 0.04	< 0.2	0.17	0.88	< 0.1	< 0.2	< 0.005	< 0.02	3.6	< 0.01	0.08	< 0.02	< 0.02	nd	nd
15	Acqua Gialla	0.19	0.01	0.12	< 0.04	< 0.2	0.002	0.04	< 0.1	< 0.2	0.006	< 0.02	0.57	< 0.01	0.01	nd	nd	nd	nd
16	Acqua Passante 1	0.18	0.02	0.24	< 0.04	< 0.2	0.019	0.04	< 0.1	< 0.2	< 0.005	9.8	0.12	< 0.01	0.63	nd	nd	nd	nd
17	Acqua Passante 2	0.26	0.01	0.42	< 0.04	< 0.2	0.08	0.37	< 0.1	< 0.2	< 0.005	0.67	0.09	< 0.01	< 0.002	nd	nd	nd	nd
21	Galleria Casanova	0.44	0.01	0.33	< 0.04	< 0.2	0.08	15.7	< 0.1	< 0.2	< 0.005	0.03	0.72	< 0.01	< 0.002	0.030	0.8	nd	nd
22	Putizza Rondinaia	< 0.1	0.03	< 0.1	< 0.04	< 0.2	0.028	0.36	< 0.1	< 0.2	< 0.005	10.1	26.4	< 0.01	< 0.002	nd	1.2	nd	nd
23	Galleria Nuova Italia	0.21	0.05	0.74	0.08	< 0.2	0.02	0.43	< 0.1	< 0.2	< 0.005	26.2	10.1	0.006	0.29	nd	nd	nd	nd
24	Tre Case	< 0.1	< 0.01	< 0.1	< 0.04	< 0.2	0.031	0.1	< 0.1	< 0.2	< 0.005	0.04	0.07	< 0.01	< 0.002	nd	nd	nd	nd
25	Acqua Salata	1.6	1.7	1.8	< 0.04	< 0.2	0.04	5.6	0.57	0.3	0.008	< 0.02	0.1	0.65	0.006	< 0.02	nd	nd	nd
26	Pian delle Borrelle	0.18	< 0.01	< 0.1	< 0.04	< 0.2	0.05	0.7	< 0.1	< 0.2	< 0.005	0.13	0.16	0.002	0.006	nd	nd	nd	nd
27	La Tagliata	< 0.1	< 0.01	< 0.1	< 0.04	< 0.2	0.02	0.64	< 0.1	< 0.2	< 0.005	0.03	< 0.01	< 0.01	0.04	nd	< 0.02	nd	nd
28	La Vena	0.22	0.02	0.15	0.04	< 0.2	< 0.01	0.06	< 0.1	0.2	0.014	< 0.02	0.05	< 0.01	0.03	nd	nd	nd	nd
29	Il Pino	0.14	0.02	0.2	0.04	< 0.2	0.004	0.1	< 0.1	< 0.2	0.008	0.05	0.04	0.001	0.009	nd	nd	nd	nd
30	Acqua Forte Ontani	0.16	< 0.01	< 0.1	< 0.04	< 0.2	0.004	< 0.04	< 0.1	< 0.2	0.009	< 0.02	< 0.01	0.005	< 0.002	nd	nd	nd	nd
31	Capo Vetra	0.59	< 0.01	< 0.1	< 0.04	< 0.2	< 0.01	0.05	< 0.1	< 0.2	< 0.005	< 0.02	< 0.01	< 0.01	0.007	nd	nd	nd	nd
32	Pozzo Hotel Aiole	< 0.1	0.03	< 0.1	0.1	< 0.2	0.01	0.39	< 0.1	0.2	< 0.005	< 0.02	0.02	< 0.01	0.025	nd	nd	nd	nd

41	Podere Fogarone	0.2	< 0.01	< 0.1	< 0.04	< 0.2	0.019	0.73	< 0.1	< 0.2	< 0.005	< 0.02	0.08	< 0.01	< 0.002	nd	< 0.02	nd	nd
42	Solforica Riguardello	< 0.1	< 0.01	1.2	< 0.04	< 0.2	0.015	3.5	< 0.1	< 0.2	0.070	0.02	0.14	< 0.01	< 0.002	nd	2.0	nd	nd
43	Fontaccia	< 0.1	< 0.01	< 0.1	< 0.04	< 0.2	0.011	0.07	< 0.1	< 0.2	< 0.005	< 0.02	< 0.01	< 0.01	< 0.002	nd	nd	nd	nd
44	Acquanera	< 0.1	< 0.01	< 0.1	< 0.04	< 0.2	< 0.01	0.17	< 0.1	< 0.2	< 0.005	< 0.02	< 0.01	0.08	0.016	nd	nd	nd	nd
45	Acqua Bolle S.Antonio	0.15	0.11	< 0.1	< 0.04	< 0.2	0.5	1.3	0.2	< 0.2	< 0.0052	< 0.02	0.06	< 0.01	0.003	nd	< 0.02	nd	nd
46	La Pigna	< 0.1	< 0.01	0.14	< 0.04	< 0.2	< 0.01	0.1	< 0.1	< 0.2	< 0.005	< 0.02	< 0.01	< 0.01	< 0.002	nd	< 0.02	nd	nd
48	Acqua Frizzante	0.24	0.1	< 0.1	< 0.04	< 0.2	0.42	0.51	< 0.1	< 0.2	< 0.005	0.04	2.1	< 0.01	< 0.002	nd	< 0.02	− 6.78	− 40.2
49	Acqua Puzzola Funina	0.9	0.25	1.3	< 0.04	< 0.2	0.022	1.18	0.11	< 0.2	< 0.005	0.04	0.02	0.01	< 0.002	< 0.02	8.7	− 6.52	− 39.6
50	Fosso Belagaio	0.2	< 0.01	0.1	< 0.04	< 0.2	0.011	0.04	< 0.1	< 0.2	< 0.005	1.6	18.6	nd	0.016	nd	< 0.02	nd	nd
51	Fosso Arlecchino	< 0.1	< 0.01	< 0.1	< 0.04	< 0.2	< 0.01	0.06	0.14	< 0.2	0.010	< 0.02	0.02	< 0.01	0.005	nd	< 0.02	nd	nd
53	Acqua Rossa	0.3	< 0.01	0.3	< 0.04	< 0.2	< 0.01	0.17	0.16	< 0.2	0.020	0.06	< 0.01	< 0.01	< 0.002	nd	nd	nd	nd
54	Badia Ardenghesca	< 0.1	< 0.01	0.2	< 0.04	< 0.2	0.015	3.7	0.2	< 0.2	0.010	0.02	< 0.01	0.015	< 0.002	nd	< 0.02	nd	nd
55	Fiume Farma	< 0.1	< 0.01	0.1	< 0.04	< 0.2	0.052	1.8	< 0.1	< 0.2	0.010	< 0.02	< 0.01	0.03	0.009	nd	< 0.02	nd	nd
56	Fiume Farma	1.6	< 0.01	0.3	0.08	< 0.2	0.22	2.6	0.23	< 0.2	0.010	0.23	0.1	< 0.01	< 0.002	nd	nd	nd	nd
57	Fiume Bardellone	< 0.1	< 0.01	0.2	< 0.04	< 0.2	0.036	2.7	< 0.1	< 0.2	0.010	0.02	< 0.01	< 0.01	< 0.002	nd	nd	nd	nd
58	Fiume Merse	< 0.1	< 0.01	0.9	< 0.04	< 0.2	0.013	4.7	< 0.1	< 0.2	0.010	< 0.02	< 0.01	0.02	0.007	nd	nd	nd	nd
59	Case Ropole	46.4	1.7	< 0.1	0.06	< 0.2	0.14	15.5	15.0	5.7	0.010	0.02	6.7	< 0.01	< 0.002	nd	nd	nd	nd
63	Le Croste	< 0.1	< 0.01	0.31	< 0.04	< 0.2	0.015	0.64	0.22	< 0.2	0.010	< 0.02	< 0.01	< 0.01	< 0.002	< 0.02	nd	− 6.14	− 36.2
68	Fonte delle Piane	0.2	< 0.01	0.22	< 0.04	< 0.2	0.047	0.34	0.19	< 0.2	< 0.005	0.02	< 0.01	< 0.01	< 0.002	nd	nd	− 6.89	− 40.4
69	Fontacce	< 0.1	< 0.01	0.69	< 0.04	< 0.2	0.066	0.65	< 0.1	< 0.2	0.090	< 0.02	< 0.01	< 0.01	< 0.002	nd	nd	nd	nd
70	Campo delle Pozze	0.4	0.02	nd	< 0.04	< 0.2	0.014	0.05	0.18	< 0.2	< 0.005	< 0.02	< 0.01	0.007	< 0.002	nd	nd	nd	nd
73	Podere S.Giuseppe	< 0.1	0.03	0.76	< 0.04	< 0.2	0.014	2.4	2.1	< 0.2	< 0.005	< 0.02	0.12	0.031	< 0.002	nd	nd	− 6.11	nd
74	Vergheria	< 0.1	< 0.01	0.38	< 0.04	< 0.2	0.054	0.61	0.4	< 0.2	0.005	< 0.02	< 0.01	0.003	< 0.002	nd	nd	− 5.87	nd
75	Pozzo irriguo 2	< 0.1	< 0.01	0.14	< 0.04	< 0.2	0.024	0.23	0.33	< 0.2	< 0.005	< 0.02	< 0.01	0.022	0.24	nd	nd	nd	nd
76	Lago Scuro	0.54	0.01	0.26	< 0.04	< 0.2	0.13	2.4	0.96	< 0.2	< 0.005	0.1	0.04	0.008	< 0.002	nd	nd	nd	nd
77	Lago Acquato	< 0.1	0.01	0.56	< 0.04	< 0.2	0.056	0.7	0.94	< 0.2	< 0.005	< 0.02	< 0.01	0.004	< 0.002	nd	nd	nd	nd
78	Lago Cerro Sughero	0.14	< 0.01	0.42	< 0.04	< 0.2	0.066	0.34	0.97	< 0.2	< 0.005	< 0.02	< 0.01	0.004	< 0.002	nd	nd	nd	nd
79	Pozzo Campolungo	< 0.1	0.02	0.42	< 0.04	< 0.2	0.03	1.2	1.8	< 0.2	< 0.005	< 0.02	< 0.01	< 0.01	0.23	nd	nd	nd	nd

All elements in mg/kg.
Al(t) = total alluminium; Al(m) = monomeric alluminium.
$\delta^{18}O$ and δD in permil vs. SMOW.
nd = not determined.

(Marini et al., 1986). Although circulating in the same geological formations, most geothermal fluids have a lower Sr content (< 7 mg/kg) with respect to the thermal springs (generally > 10 mg/kg, Fig. 3). This is due to the fact that Sr tends to coprecipitate with Ca during gypsum and calcite precipitation at high temperature in response to variations of CO_2 partial pressure (Marini and Chiodini, 1994).

Barium, which crystallochemically behaves like Sr, has a higher content in the cold shallow springs than in the thermal waters and this can be explained with the precipitation of barite inside the Mesozoic formations, due to the large concentration of SO_4 ions in the thermal waters from the dissolution of anhydrite. This agrees well with the saturation indexes calculated for relevant minerals using WATEQ 4F (Ball and Nordstrom, 1991) program, indicating that most of thermal samples are barite saturated. Moreover, dispersed barite ore deposits occur in the Mesozoic limestone in several areas of southern Tuscany (Tanelli, 1983; Ceccarelli et al., 1989).

Bromine is geochemically correlated with Cl and a Br vs. Cl diagram (Fig. 5) can be used to determine if those Cl-rich thermal samples emerging at the boundaries of the carbonate reservoir formation are genetically related to recent unmodified marine

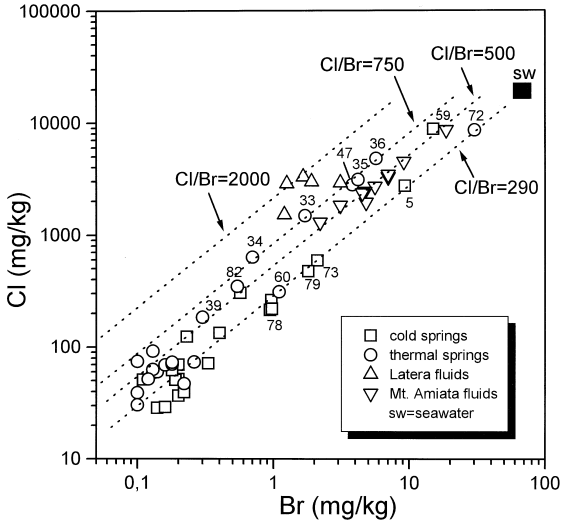

Fig. 5. Bromine vs. Cl diagram. Dilution lines with fresh seawater (Cl/Br = 290) and springs from the Siena basin (Cl/Br = 750) and geothermal fluids from Mt. Amiata (Cl/Br = 500) and Latera (Cl/Br = 2000) are shown.

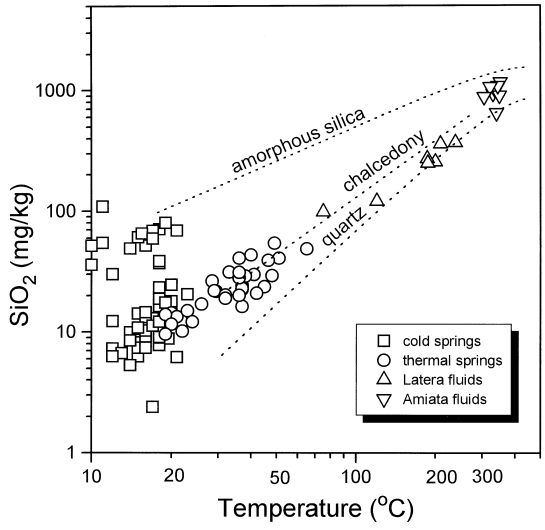

Fig. 6. Silica vs. sampling temperature (°C) diagram.

(Cl/Br = 290) waters, to modified fossil waters, or to high salinity Cl-rich (magmatic?) fluids. Only sample #72 emerging close to the Tyrrhyenian shoreline, a few cold waters close to sample #72 (#73, #78, #79), and sample #5 in the Siena basin have Cl/Br ratio close to that of seawater. In contrast, thermal spring waters #33, #35, #36 and #47 and cold sample #59 (all emerging in the Siena basin, Fig. 1) have the Cl/Br ratio ranging from 500 to 750, suggesting a marine end-member mixed with geothermal fluids. High Cl/Br ratios are measured for the geothermal fluids from deep wells at Mt. Amiata and Latera, having Cl/Br ratios as high as 500 and 2000, respectively (Fig. 5).

The concentration of silica in thermal springs (20–50 mg/kg) and in most cold springs (5–15 mg/kg) suggests that this compound is equilibrated at depth with chalcedony (Fournier, 1973) at temperatures close to those measured at the emergence (Fig. 6). This implies long circulation underground (Duchi et al., 1987a, 1992), that is also confirmed by the absence of radiogenic tritium in these springs (Celati et al., 1991; Battaglia et al., 1992). As observed in other volcanic products, silica content in cold waters circulating within the Mt. Amiata volcanic edifice plot along with the amorphous silica solubility curve (Fournier, 1973), whereas geothermal well waters

Table 4
Minor, trace, and isotopic data in thermal springs emerging from the carbonate reservoir

No.	Name	NH_4	Li	F	Rb	Cs	Ba	Sr	Br	I	As	Al(t)	Fe	Sb	Zn	Al(m)	H_2S	$\delta^{18}O$	δD
1	Bagnaccio S.G.Asso	0.45	0.2	1.5	0.04	< 0.2	0.014	12.1	0.13	0.2	< 0.005	0.02	0.14	0.008	0.021	< 0.02	nd	7.7[a]	nd
6	Cava Solet	0.14	0.24	1.8	0.05	< 0.2	0.011	12.3	0.14	< 0.2	< 0.005	0.03	< 0.01	< 0.01	< 0.002	< 0.02	nd	nd	nd
7	Bagno Vignoni	0.56	0.25	1.6	< 0.04	< 0.2	0.012	12.4	0.13	< 0.2	< 0.005	0.03	0.17	< 0.01	< 0.002	nd	nd	7.9[a]	nd
18	Bagni S.Filippo	2.6	0.23	0.94	< 0.04	< 0.2	0.019	14.0	< 0.1	< 0.2	0.047	0.22	< 0.01	0.018	< 0.002	0.22	2.2	8.2[a]	53.2[a]
19	Passante S.Filippo	0.12	0.11	1.5	< 0.04	< 0.2	0.02	11.3	< 0.1	< 0.2	0.015	< 0.02	< 0.01	0.012	< 0.002	< 0.02	nd	nd	nd
20	Fosso bianco	1.6	0.2	1.3	< 0.04	< 0.2	0.019	11.5	< 0.1	< 0.2	0.034	0.03	< 0.01	< 0.01	< 0.002	nd	1.5	nd	nd
33	Doccio bis	10.0	2.9	1.8	0.24	0.25	0.32	13.3	1.7	< 0.2	0.610	0.04	0.1	< 0.01	0.004	0.15	8.5	6.0	40.8
34	Bagnolo di Montisi	3.9	1.4	1.4	0.13	< 0.2	0.014	10.2	0.7	< 0.2	0.100	0.01	0.23	0.017	< 0.002	< 0.02	9.0	6.5	42.3
35	Mortaione	88.8	18.8	1.7	2.1	1.70	9.8	13.1	4.2	0.4	0.010	0.04	0.01	< 0.01	< 0.002	< 0.02	< 0.02	2.1	42.8
36	Acqua Borra	28.4	19.7	1.2	0.81	0.71	0.047	11.6	5.7	1.1	0.01	0.46	9.6	< 0.01	< 0.002	0.05	< 0.02	5.3	44.7
37	Caldanelle	0.12	0.04	1.6	< 0.04	< 0.2	0.022	10.3	< 0.1	< 0.2	0.010	0.4	0.04	0.19	< 0.002	< 0.02	1.3	6.7	41.0
38	Molin del Tifo	< 0.1	0.02	1.4	< 0.04	< 0.2	0.011	8.5	< 0.1	< 0.2	0.010	< 0.02	< 0.01	< 0.01	< 0.002	< 0.02	< 0.02	6.4	39.1
39	Petriolo	4.4	1.1	1.2	0.14	< 0.2	0.024	12.3	0.3	< 0.2	< 0.005	0.07	0.03	< 0.01	< 0.002	< 0.02	17.5	6.4	38.6
40	Macereto	0.3	0.11	0.7	< 0.04	< 0.2	0.023	5.1	< 0.1	< 0.2	< 0.005	0.02	< 0.01	< 0.01	< 0.002	nd	1.5	nd	nd
47	Guado di Pietrafessa	71.8	17.7	1.2	1.8	1.50	1.6	3.1	3.8	0.4	< 0.005	0.06	2.1	< 0.01	< 0.002	nd	nd	3.0	41.1
52	Podere Pratella	1.4	0.21	1.4	< 0.04	< 0.2	0.42	10.3	0.12	< 0.2	0.020	0.16	0.55	< 0.01	< 0.002	nd	< 0.02	nd	nd
60	Alberese	0.24	0.24	1.1	< 0.04	< 0.2	0.023	6.8	1.1	< 0.2	< 0.005	0.02	0.17	0.003	< 0.002	< 0.02	1.5	6.3	40.8
61	Bagni di Saturnia	30.7	0.53	2.0	0.04	0.04	0.022	11.3	0.16	< 0.2	0.030	0.02	< 0.01	< 0.01	< 0.002	< 0.02	9.0	6.9	41.5
62	Pozzo Irriguo	2.6	0.66	1.2	0.08	< 0.2	0.032	8.5	0.18	< 0.2	0.080	< 0.02	74.6	0.003	0.03	< 0.02	1.3	6.9	41.8
64	Poggio Cavallucciaro	0.22	0.02	1.7	< 0.04	< 0.2	0.011	9.1	0.26	< 0.2	0.020	< 0.02	< 0.01	0.004	< 0.002	nd	6.1	nd	nd
65	Lasco delle Vene	0.11	< 0.01	1.4	< 0.04	< 0.2	0.012	6.5	0.22	< 0.2	0.02	< 0.02	< 0.01	0.05	0.03	nd	nd	nd	nd
66	Scarceta	1.1	0.02	2.2	< 0.04	< 0.2	< 0.01	11.4	0.1	< 0.2	0.030	< 0.02	0.24	0.002	< 0.002	< 0.02	3.0	6.5	nd
67	Le Caldine	32.1	0.62	2.1	0.05	< 0.2	0.017	10.1	0.18	< 0.2	0.032	0.02	0.09	< 0.01	< 0.002	< 0.02	2.2	nd	nd
71	Galleria Morone	0.16	0.02	1.1	< 0.04	< 0.2	< 0.01	5.8	< 0.1	< 0.2	0.010	0.03	< 0.01	0.004	< 0.002	nd	1.8	nd	nd
72	Bagni dell' Osa	8.4	0.42	2.2	0.07	0.27	0.015	18.5	30.2	< 0.2	0.015	< 0.02	0.08	0.002	< 0.002	< 0.02	12.4	4.1	22.0
80	Bagni Galleraie	8.3	0.03	1.56	< 0.04	nd	0.25	11.75	< 0.1	nd	0.09	0.09	0.82	0.001	< 0.002	0.05	nd	6.4	40.8
81	Vene di Ciciano	< 0.1	0.02	0.88	< 0.04	< 0.2	0.03	5.3	< 0.1	nd	< 0.005	< 0.02	< 0.01	< 0.01	0.05	< 0.02	nd	7.2	47.0
82	Rapolano	3.3	1.3	2.09	0.16	0.07	0.05	18.04	0.54	nd	< 0.005	0.02	0.58	< 0.01	< 0.002	nd	2.5	7.5[a]	44.1[a]
83	Chianciano Terme	nd	0.05	2.85	< 0.04	nd	nd	11.88	< 0.1	nd	nd	nd	nd	0.016	nd	nd	nd	7.7[a]	nd
84	Sarteano	< 0.1	0.02	1.27	< 0.04	nd	nd	7.92	< 0.1	nd	nd	nd	nd	nd	nd	nd	nd	7.7[a]	nd
85	S.Casciana Bagni	0.5	0.07	1.56	0.01	0.05	0.04	11.0	0.13	nd	< 0.005	< 0.02	0.08	< 0.01	0.002	nd	< 0.02	7.7[a]	nd
86	Pitigliano	0.36	0.01	3.04	< 0.04	< 0.2	0.011	11.1	< 0.1	nd	< 0.005	< 0.02	0.2	0.011	< 0.005	nd	nd	6.7[b]	40.5[aa]
87	Canino	0.81	0.37	2.47	0.12	< 0.2	0.03	13.1	0.1	nd	0.11	< 0.02	0.03	< 0.01	< 0.005	nd	nd	7.0[b]	38.2[a]
88	Bagnaccio	0.14	0.13	3.61	0.13	0.12	0.04	12.3	< 0.1	nd	0.18	0.07	< 0.01	< 0.01	< 0.005	nd	nd	6.3	37.0
89	Roselle	0.23	0.04	1.22	< 0.04	< 0.2	< 0.01	11.0	0.1	nd	< 0.005	< 0.02	< 0.01	< 0.01	< 0.002	< 0.02	nd	5.2	32.6

All elements in mg/kg.
Al(t) = Total alluminium; Al(m) = Monomeric alluminium.
$\delta^{18}O$ and δD in permil vs. SMOW.
nd = not determined.
[a]data after Fancelli and Nuti (1975).
[b]data after D'Amore et al. (1979).

Table 5
Chemical composition of fluids from geothermal wells

Name	*t*	pH	TDS	Ca	Mg	Na	K	HCO_3	Cl	SO_4	B	SiO_2	NH_4	F	Ba	Sr	Br
Latera 3d	238	5.91	9780	2.75	0.22	2740	500	1317	2890	1380	579	371	23.2	25	0.06	0.45	1.25
Latera 2	209	5.4	7477	17.3	1.2	2240	320	975	2940	360	262	362	25.5	10.3	0.2	1.4	3.1
Latera 4	200	5.84	6177	15.3	1.1	1760	285	1240	1840	585	194	257	54	15.3	nd	0.04	nd
Vulsini 2	120	5.36	6243	25.4	14.8	1698	342	1080	1531	1150	281	121	16.9	5.4	0.04	1.1	1.2
Latera SGH1	186	5.71	7092	23.6	3.5	2360	153	681	3315	157	126	273	42.6	6.5	0.13	5.1	1.65
Latera G2	187	5	6796	12	2.6	2120	286	636	3000	250	239	250	17.6	6.8	0.13	2.9	1.9
Latera 14	75	6.35	3217	614	77.5	74	94.5	1105	116	1010	27.6	99	33	nd	0.3	14.3	nd
Amiata 16b	351	6.78	21596	73.6	0.21	4660	1280	1831	8660	0.5	3932	1160	290	16.2	0.25	0.52	18.7
Amiata 26	330	6.94	8885	6	0.03	1530	292	604	2380	12.5	3128	933	79	7.3	0.028	0.1	4.5
Amiata 27	335	7.78	6317	2.4	0.02	1200	208	653	1840	3	1401	1010	95	4.9	0.01	0.03	3.1
Amiata 27b	349	8.23	3072	8.6	0.35	532	76.8	665	585	42	262	900	81	5.6	0.06	0.13	0.9
Amiata 33	344	6.78	12786	12.1	0.41	2870	420	1403	4420	18.7	3460	182	108	3.9	0.13	0.7	8.5
Amiata 33A	321	7.62	5056	3.6	0.19	575	106	560	1120	0.5	1632	1060	216	nd	0.02	0.03	2
Amiata 36	305	8.12	3466	7.2	0.45	564	92.3	495	894	30.6	508	875	110	5.8	0.02	0.06	1.8
Amiata 36b	340	8.31	3055	27.4	4	597	116	516	773	188	190.5	643	53	3	0.1	0.22	1.3

Temperature (t) in °C; total dissolved solids (TDS) and all elements in mg/kg.
Data for Latera and Vulsini are from Gianelli and Scandiffio (1989).
nd = not determined.

from Latera plot along the solubility curve for quartz at bottom hole temperatures.

Ammonium and B have a large variability in both the thermal (0.1–88 and 1–800 mg/kg, respectively) and cold (0.1–46 and 0.1–185 mg/kg, respectively) springs. They are generally correlated with Cl due to the presence of a marine-originated endmember as already observed in other areas of central Italy (Bencini and Duchi, 1986). Ammonium and B show a positive correlation in both the thermal spring waters and geothermal fluids (Fig. 7) suggesting their common origin, and that thermal springs from the Siena basin (#35, #36 and #47) might leak from undiscovered geothermal fluids rich in B and NH_4.

4.3. Gas compositions

Major and minor components of gases from thermal and cold springs as well as dry vents are reported in Table 6. Carbon dioxide is the main component among the gases in the cold springs and/or dry vents (> 85–90%), while N_2 is generally very abundant (> 50%) in the gas phase associated with the thermal springs (Duchi and Minissale, 1995).

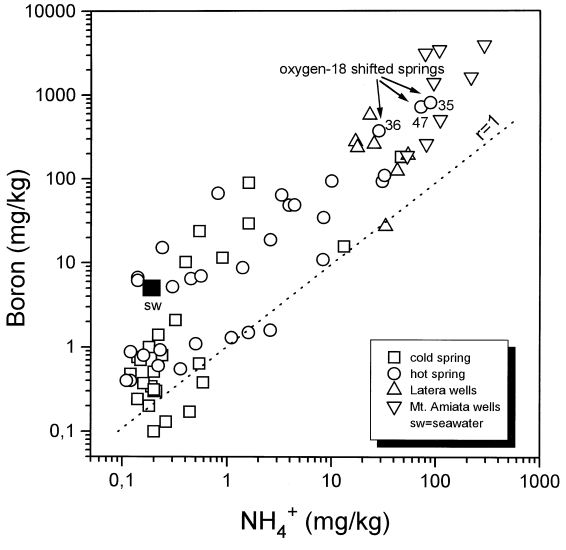

Fig. 7. Boron vs. NH_4 diagram. Spring waters emerging in the Siena basin, which have a relevant shift in oxygen-18 (Fig. 9), have similar NH_4 and B concentrations with those of fluids discharging from geothermal wells.

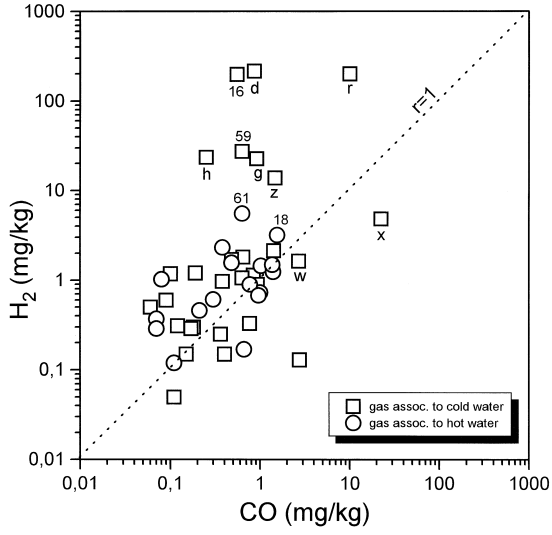

Fig. 8. Hydrogen vs. CO diagram in the sampled gases.

The gases from dry vents, generally emerging from the cap-rock formations, are rich in CH_4 with a maximum of 13% by vol. (sample #h), whereas it is < 2.2% in the gases associated with cold water and generally < 0.6% in the gases associated with the thermal springs emerging at the boundary of the carbonate reservoir rocks. This suggests that CH_4 prevalently forms at shallow level underground above the Mesozoic limestone formations, and/or, if derived from inside or below the reservoir, it solubilizes at a higher H_2O/gas ratio when associated with the regional thermal aquifer.

The maximum H_2S concentration in the gases is 1.2%, but a clear discrimination between those in 'cold' and 'thermal' gases has not been observed. Thus, similar origin of H_2S might be suggested for both the two groups (e.g. alteration of pyrite, sulphate reduction, bacteria activity ..., etc.). However, when considering the high reactivity and solubility of H_2S in shallow aquifers, it is unlikely that the measured concentration at surface would reflect the real H_2S content at depth.

Concentration of H_2 and CO, whose high values are good indicators of high temperature at depth (Tonani, 1973; Giggenbach, 1980; Bertrami et al., 1985), are low in most of gases including the high-temperature samples from Travale, Mt. Amiata and

Table 6
Chemical and isotopic composition of gas samples

No.	Name	H_2	O_2 + Ar	N_2	CH_4	CO_2	H_2S	CO	C_2H_6	He	Rn	$\delta^{13}C$	$\delta^{15}N$	$^3He/^4He$	$^{40}Ar/^{36}Ar$
1	Bagnaccio S.G. Asso	1.45	0.2718	7.600	0.0098	91.60	< 0.0005	1.02	2.00	8.5	38.0	− 7.2	nd	nd	nd
4	Acqua Puzzola	1.72	0.1303	4.500	1.4600	95.50	< 0.0005	<	2.50	5.6	13.0	− 3.8	5.42	0.214	295
7	Bagno Vignoni	1.25	1.3050	8.600	0.0190	90.06	< 0.0005	1.39	< 2	5.8	31.0	nd	nd	nd	nd
14	Acqua Forte Bagnore	1.14	0.2852	2.150	1.6200	94.50	< 0.0005	0.84	4.80	nd	nd	nd	nd	nd	nd
16	Acqua Passante	198.00	0.0056	0.380	1.2500	98.90	0.2500	0.55	4.20	1.9	21.0	nd	nd	nd	nd
18	Terme S.Filippo	3.19	0.2484	17.500	0.0110	83.46	0.0930	1.54	< 2	9.5	nd	− 3.2	nd	nd	nd
20	Fosso bianco	0.73	0.0970	7.157	< 0.0001	92.70	0.0150	1.00	< 2	24.7	nd	nd	nd	nd	nd
22	Putizza Rondinaia	2.66	0.0055	2.600	1.3400	93.30	0.0620	<	2.60	8.8	4.8	nd	nd	nd	nd
33	Doccio	0.37	0.0586	0.772	0.0169	98.01	0.3020	0.07	nd	2.0	12.0	− 5	nd	nd	nd
33	Doccio bis	0.46	0.1020	0.944	0.0251	96.58	0.3280	0.21	nd	nd	32.8	− 5.39	nd	nd	nd
35	Mortaione bis	0.29	0.0060	0.044	0.0356	97.85	0.0220	0.07	nd	< 1	28.4	− 5.96	nd	nd	nd
35	Mortaione	1.57	0.1000	0.181	0.0030	98.12	0.0150	0.48	nd	< 1	4.5	− 6.65	nd	nd	nd
36	Acqua Borra	0.12	0.0216	0.554	0.0822	97.23	< 0.0005	0.11	nd	5.0	2.4	− 6.3	nd	0.15	nd
39	Petriolo	1.49	0.1487	0.443	0.0054	99.47	< 0.0005	1.36	< 2	< 2	256.5	− 5.5	nd	0.96	nd
40	Puzzola Macereto	1.03	0.9790	66.780	0.2990	31.16	0.9870	0.08	nd	nd	54.5	− 9.45	nd	nd	nd
45	Acquabolle S.Antonio	0.30	0.0831	0.856	2.1300	94.24	0.0010	0.18	nd	nd	8.5	− 5.35	nd	nd	nd
47	Pietrafessa	0.50	0.0172	0.037	0.0080	97.78	0.0024	0.06	nd	nd	1.7	nd	nd	nd	nd
52	Pratella	0.17	1.0290	63.850	0.1320	33.68	0.0044	0.66	nd	nd	nd	nd	nd	nd	nd
59	Case Ropole	27.30	0.0368	0.469	0.4850	97.43	< 0.0005	0.63	nd	nd	3.5	nd	nd	nd	nd
61	Saturnia	5.56	0.3400	64.000	0.4800	34.24	0.1800	0.63	< 2	19.0	12.3	− 6.4	0.57	0.48	295
64	P.gio Cavallucciaro	0.61	0.4500	92.920	< 0.0001	5.02	0.0640	0.30	< 2	21.0	nd	nd	nd	nd	nd
71	Galleria Morone	0.90	2.9800	37.750	40.4200	19.41	0.0040	0.77	nd	6.2	18.4	nd	nd	nd	nd
72	Bagni dell' Osa	0.68	0.5090	78.720	0.5480	20.41	0.4200	0.96	< 2	95.0	354.0	− 9.57	0.69	0.095	305
82	Rapolano	< 1	0.0688	0.650	0.0020	99.64	0.0380	< 10	< 2	< 2	nd	− 7.9	nd	0.09	nd
85	S.Casciana Bagni	< 2	1.9437	91.187	0.0415	6.95	< 0.0005	< 10	< 2	31.0	nd	− 8.62	nd	0.04	nd
88	Bagnaccio Viterbo	2.32	0.1000	0.390	0.0150	98.78	0.1660	0.38	nd	< 2	29.6	− 1.7	nd	0.54	293
89	Roselle	< 1	5.8111	89.341	0.0006	5.39	< 0.0005	nd	< 2	< 2	nd	− 9.56	nd	0.065	295
a	Bagnolo dell' abate	1.11	0.0406	6.800	3.5800	89.99	< 0.0005	< 10	21.00	18.5	5.0	nd	nd	nd	nd
b	Puzzole Zancona	0.90	0.0084	0.710	5.7600	94.80	0.2670	0.93	14.80	1.6	28.0	− 4.64	3.77	0.46	325
c	Puzzole di Bagnore	1.47	0.0384	0.510	2.4600	96.01	< 0.0005	< 10	8.00	0.9	28.0	− 2.0	nd	nd	nd
d	Elmeta	215	0.0147	0.680	2.0600	96.01	0.2500	0.86	8.00	2.5	19.0	nd	nd	nd	nd
e	Fosso Olivo	1.81	0.0191	2.300	1.7650	99.10	0.1420	0.64	< 2	7.5	nd	− 3.33	4.77	0.134	328
f	Putizza Pietrineri	1.06	0.0062	2.240	1.5000	99.40	0.1720	0.63	3.50	7.7	15.0	nd	nd	nd	nd
g	Casa Voltole	22.70	0.0117	2.170	0.6400	96.90	< 0.0005	0.91	99.50	13.8	41.0	nd	nd	nd	nd
h	Zolfinaia	23.40	0.1100	14.330	13.1700	72.37	0.6380	0.25	nd	nd	40.7	− 3.44	nd	nd	nd
i	Fosso Solfare	2.14	10.1500	40.430	0.4860	55.52	0.0660	1.41	nd	nd	31.4	− 5.26	nd	nd	nd
j	Casa Monti	0.60	0.0381	10.840	8.3900	80.47	0.2580	0.09	nd	nd	23.4	− 4.27	nd	nd	nd

k	Frana	0.31	0.0518	4.330	0.1130	94.00	0.0414	0.12	nd	nd	15.7	−4.92	nd	nd	nd
l	Fontazzi	0.25	0.0250	8.900	3.2700	86.36	0.1650	0.36	nd	nd	23.4	nd	nd	nd	nd
m	Le Palaie	0.15	0.0136	3.050	2.9500	92.73	0.2360	0.15	nd	nd	32.1	−3.83	nd	nd	nd
n	Monterosso	0.05	0.0760	< 0.0001	< 0.0001	98.63	0.0020	0.11	nd	0.7	7.7	nd	nd	nd	nd
o	Petricci	nd	0.0450	4.600	4.1500	89.76	0.2110	nd	nd	1.3	14.2	nd	nd	nd	nd
p	Banditella	1.20	0.0320	5.200	3.3800	90.28	0.0270	0.19	nd	1.5	11.2	nd	nd	nd	nd
q	Anteie	0.33	0.0940	17.860	6.0100	77.92	0.0250	0.76	nd	2.7	9.8	nd	nd	nd	nd
r	Selvena	200	0.0050	1.150	6.1900	92.12	1.1900	10.00	nd	3.2	15.5	−4.9	4.43	0.414	317
s	S.Martino Fiora 1	0.29	0.0090	0.670	0.1910	99.33	0.0250	0.17	nd	3.4	9.9	0.14	5.02	0.686	nd
t	S.Martino Fiora 2	0.97	0.0120	0.680	0.2060	98.81	0.0040	0.38	nd	3.6	30.4	nd	nd	nd	nd
u	Tafone sud	0.15	0.1850	23.350	0.0800	74.67	0.0070	0.40	nd	18.0	9.0	−3.81	nd	0.38	295
v	Solfiere di Pereta	0.13	7.5600	70.010	0.4390	21.44	0.0040	2.74	nd	5.0	6.0	−6.27	−0.2	0.049	295
w	Torre Alfina	1.63	0.0780	1.040	0.1700	99.64	0.0630	2.68	nd	8.0	66.6	0.4	nd	0.26	295
x	Bolsena	4.85	0.0800	0.260	0.0140	99.88	0.0020	22.30	nd	nd	38.9	1.7	nd	nd	nd
y	Cimitero di Guerra	1.53	0.2000	4.400	0.0044	95.47	nd	nd	nd	nd	1310	nd	nd	nd	nd
z	Morticini	13.90	0.0600	1.120	0.1460	99.44	0.1160	1.46	nd	nd	227.0	nd	nd	nd	nd
aa	Montefiascone	1.69	0.1100	6.200	1.0100	94.09	nd	nd	nd	nd	nd	1.6	nd	nd	nd
ab	Campeggio	1.51	0.0970	7.240	0.0047	94.00	nd	nd	nd	nd	nd	nd	nd	nd	nd
ac	Solfatara Celleno	1.40	0.0630	3.960	0.6330	96.71	nd	nd	nd	3.0	28.0	−0.32	nd	0.56	306
ad	Castel di Broco	1.18	0.4500	18.570	0.2750	80.63	0.0020	0.10	nd	nd	484.0	1.92	nd	0.42	295
ae	Le Puzzolaie	1.70	0.1100	1.090	0.0910	97.71	0.5300	0.48	nd	13.0	268.0	1.31	nd	0.48	297
af	Acquaforte	1.56	1.0400	53.490	< 0.0001	44.76	nd	nd	nd	nd	nd	nd	nd	nd	nd
ag	Pantella 192	1.88	0.0640	4.210	0.1620	96.68	nd	nd	nd	nd	nd	nd	nd	nd	nd
ah	S.M. dell'Aquila	2.88	1.7100	93.220	0.0196	9.08	nd	nd	nd	nd	33.3	nd	nd	nd	nd
ai	Monterozzi	< 2	0.0174	1.401	0.1348	98.41	0.6520	< 10	< 2	2.0	nd	−0.1	nd	0.35	295
aj	Tuscania	< 2	0.0149	1.631	0.0401	97.12	0.7894	< 10	< 2	2.0	nd	0.1	nd	nd	nd
ak	Palazzo al Piano	454	0.0332	6.745	6.5750	85.78	0.4400	< 10	43.00	46.0	nd	−4.66	5.51	1.81	295
al	Castelletto	< 2	0.2268	2.796	4.0991	92.78	0.2400	< 10	25.00	24.0	nd	−4.31	5.54	1.35	295
am	Torrite di Siena	< 2	0.9550	8.501	1.5998	88.36	< 0.0005	< 10	< 2	24.0	nd	−3.87	6.13	0.11	295
an	S.Albino	< 2	0.7689	4.899	0.6301	94.76	< 0.0005	< 10	< 2	20.0	nd	−5.2	2.89	0.162	295

O_2 + Ar, N_2, CH_4, CO_2, H_2S in % by vol.; H_2, CO, C_2H_6, He in ppm (vol); Rn in BI/l; $\delta^{13}C$ and $\delta^{15}N$ in permil.
$^3He/^4He$ as R/R_A ($R/R_A = {}^3He/{}^4He(sample)/{}^3He/{}^4He(air)$).
$^{13}C/^{12}C$ isotopic ratios in CO_2 from Panichi and Tongiorgi (1976).
$^{15}N/^{14}N$ ratios in N_2 are from Minissale et al. (1995).
$^3He/^4He$, $^{40}Ar/^{36}Ar$ and He/Ne ratios are from Minissale et al. (1997).

Latera geothermal fields. They show a positive correlation in both thermal and cold gases (Fig. 8). The only samples which plot off the general trend are some of those in the Mt. Amiata area where H_2 is about 200 mg/kg (samples #16, #d, #r; Table 6). Reservoir temperatures of 200–250°C are calculated for these samples with the H_2–H_2S–CH_4–CO_2 (D'Amore and Panichi, 1980) and H_2/Ar (Giggenbach, 1991) geothermometers.

5. Stable isotopic composition

5.1. Thermal waters and geothermal well fluids

Measurements of the oxygen and hydrogen isotopic compositions have mainly been made on the Ca-SO_4 thermal samples associated with the Mesozoic carbonates. Delta ^{18}O and δD original data and data from the literature are included in Tables 3 and 4 and Fig. 9. Two samples from the Latera geothermal wells (Battaglia et al., 1992) and the #35 and #47 thermal springs located in the western margin of the Siena basin have heavy $\delta^{18}O$ values (-2.11 and -2.98‰ vs. SMOW, respectively). The remaining cold and thermal waters fall between the global meteoric (Craig, 1963) and the Mediterranean (Gatt and Carmi, 1970) meteoric water lines (Fig. 9). If we

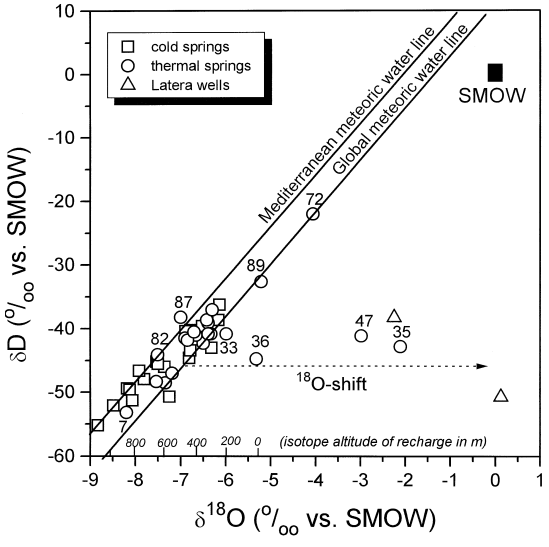

Fig. 9. $\delta^{18}O$ vs. δD diagram for some of the thermal and cold springs analysed. Isotopic values from the two Latera geothermal wells are from Battaglia et al. (1992).

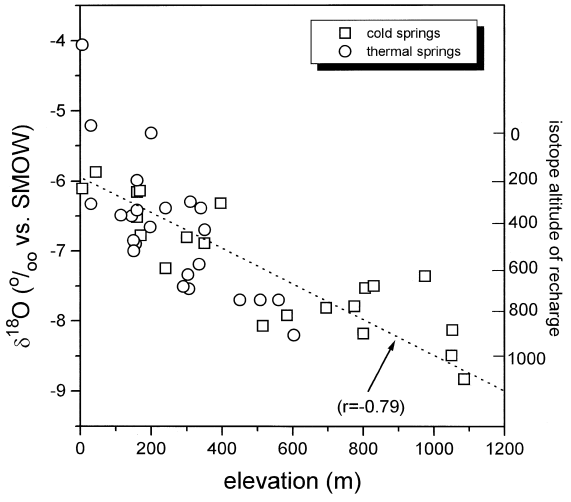

Fig. 10. $\delta^{18}O$ vs. emergence altitude for both thermal and cold springs.

consider that all the thermal spring waters related to the Italian geothermal and/or volcanic areas display a meteoric origin (Minissale, 1991a), the two thermal samples from the Siena basin must be considered a good indication of the presence of a high-enthalpy system at depth. On the basis of sample #35, Panichi (1982) hypothesized a boiling reservoir with temperatures between 150 and 200°C underneath the Siena graben, far from any of the already discovered geothermal fields.

In order to verify that waters recharging aquifers are of local meteoric origin, $\delta^{18}O$ isotopic data are plotted against the emergence altitude of springs in Fig. 10. The figure shows that the altitude of recharge areas is, in general, within the mean altitude of mountains in the investigated area (200–1000 m), which morphologically coincide with the main outcrops of the carbonate formations. The more positive $\delta^{18}O$ values coincide with the topographically lower areas close to the Tyrrenian sea, where the isotopic fractionation of ^{18}O in rain is minimal. Similarly the most fractionated $\delta^{18}O$ values have been measured in springs emerging near the Cetona ridge in the Apennines.

5.2. Isotope composition of gas samples

A detailed survey of the isotopic composition of carbon in the CO_2 gas vents in central-southern Italy was conducted in the early 70's by Panichi and

Tongiorgi (1976). Data from the previous study as well as those of the present study have been used to draw the $\delta^{13}C$ isoconcentration map in Fig. 11. Two different zones can be recognised: (1) the central-northern part where $\delta^{13}C$ values range between -4.0 and -7.0‰ (PBD); and (2) the southern part where $\delta^{13}C$ values are high with maximum of $+1.92$‰ (sample #ad). The $\delta^{13}C$ values from the southern part have recently been reinterpreted by Marini and Chiodini (1994) as the result of strong thermometamorphic processes in the Mesozoic formations with typical values of limestones ranging from -1.0 to $+2.0$‰ (Faure, 1986). In the central-northern part, the $\delta^{13}C$ values are close to those for primary carbonatitic magmas (about -5.0‰; Kyser, 1986) and they have been related to a high contribution of CO_2 from the upper mantle (Marini and Chiodini, 1994; Minissale et al., 1995). This interpretation is supported by the map of the $^3He/^4He$ [as $R/R_A = (^3He/^4He_{(sample)})/(^3He/^4He_{(air)})$] distribution in Fig. 12, where a slight enrichment of mantle ^3He in CO_2-rich samples (where $R/R_A > 0.2$; Marty et al., 1992) in most of the study area is evident, with a more pronounced enrichment in the Travale field (up to $R/R_A = 1.81$ in sample #ak, Table 7). Similar high values have been interpreted in the nearby Larderello area as due to a 20–30% contribution of He from the mantle to the total He (Hooker et al., 1985).

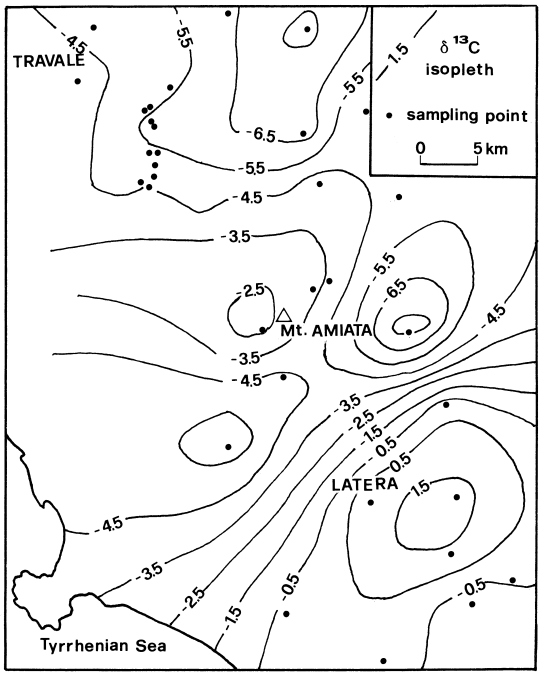

Fig. 11. $\delta^{13}C$ in CO_2 isoconcentration map (same area as in Fig. 1). See text.

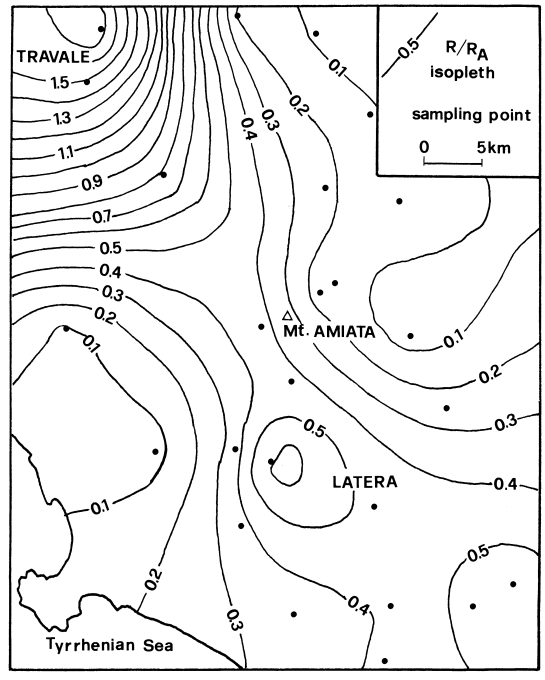

Fig. 12. $^3He/^4He$ (as R/R_A) distribution map (same area as in Fig. 1). Two samples in the Travale area show a remarkable contribution of ^3He from the mantle, probably a lateral leakage from the nearby easten part of the Larderello field (Hooker et al., 1985).

N_2-rich ($>50\%$) samples have a $\delta^{15}N$ value similar to the air ($\delta^{15}N = 0$) whereas depleted N_2 samples are strongly enriched in ^{15}N (Table 6). Since such isotopic enrichments are found for samples with $N_2/(O_2 + Ar) > 100$, they are presumably related to contributions of N_2 from the Paleozoic metamorphic basement as reported from other areas of continental margin (Jenden et al., 1988). Generally speaking, occurrence of N_2 indicates a meteoric origin, and N_2-rich gases are relatively common all over the world (Jenden et al., 1988; Giggenbach et al., 1993). This origin is very likely for the gas phase associated to the thermal springs where the mixing of cold air-saturated rainwaters coming from the reservoir

Table 7
Temperature evaluated with geothermometers in liquid phase

No.	Name	t(e)	t(calc)	t(qtz)	t(k-Mg)	t(N-K-C)	t(N-L)	t(N-L)2	t(N-K)
1	B.S.G.Asso	29.5	35	67	39	165	158	217	282
6	Cava Solet	48	47	79	46	178	156	216	306
18	B.S.Filippo	51	62	93	35	183	259	295	385
33	Doccio bis	49	76	106	77	143	138	201	201
35	Mortaione	36	62	93	135	228	255	292	254
36	A. Borra	37	39	71	121	198	190	243	163
39	Petriolo	45	38	70	54	165	240	281	248
60	Alberese	29	35	67	40	121	97	166	143
61	B. Saturnia	37	36	68	39	149	225	269	226
72	Bagni Osa	32	32	64	88	159	< 0	56	119
80	Galleraie	32	29	62	15	142	155	215	300
82	Rapolano	38	47	79	72	178	144	206	234
83	Chianciano	36	45	77	26	162	133	197	319
84	Sarteano	24	13	45	14	150	142	204	318
85	S.C.Bagni	42	33	66	15	92	79	150	111
86	Pitigliano	36	32	64	74	377	91	160	> 1000
87	Canino	40	65	96	66	191	144	206	305
88	Bagnaccio	65	71	101	64	253	163	222	616
89	Roselle	36	50	81	23	136	93	162	229

t(e) = emergence temperature; t(calc) = chalcedony (Fournier, 1973; t(qtz) = quartz (Fournier and Rowe, 1966); t(K-Mg) = K/Mg (Giggenbach et al., 1983); t(N-K-C) = Na–K–Ca (Fournier and Truesdell, 1973); t(N-L) = Na/Li (Fouillac and Michard, 1981); t(N-L)2 = Na/Li (Kharaka et al., 1982); t(N-K) = K/Na (Truesdell, 1976; Tonani, 1980; Arnorsson, 1983; Fournier, 1979; Giggenbach et al., 1983; Nieva and Nieva, 1987).

outcrops with thermal waters favours the enrichment in atmospheric nitrogen. Minissale et al. (1995) have pointed that N_2 in central Italy is also generated from the Paleozoic metamorphic formations by the oxidation of NH_4, which is common both in feldspar and mica (Honma and Itihara, 1981). Thus, two different N_2 source zones can be identified: atmospheric and metamorphic. The $\delta^{15}N$ areal distribution does not show the two different sectors observed for the $\delta^{13}C$ and $^3He/^4He$ data, probably because the high concentration of atmospheric-originated N_2 dilutes possible small contributions of the ^{15}N-enriched deep components.

$^{40}Ar/^{36}Ar$ isotopic ratios are very similar to that of the air ($^{40}Ar/^{36}Ar = 295$). Despite the large variation in the $N_2/(O_2 + Ar)$ ratio, no differences in $^{40}Ar/^{36}Ar$ have been observed for N_2-rich and N_2-poor gases. If $^{40}Ar/^{36}Ar$ ratios similar to that of the air are plausible for the N_2-rich gases, air contamination during sampling may also be invoked for the N_2-poor gases. Since the Ar content in the air is high (about 0.9%), even a small contamination can mask the actual contribution of radiogenic ^{40}Ar from the depth if: (1) the residence time of the gas phase underground is short; (2) the concentration of K is low; (3) the rate of water–rock interaction is poor. Moreover, since in central Italy several deep and shallow aquifers occur, a rising gas phase may encounter at least one meteoric-originated aquifer before emerging, and this, similarly to what happen to ^{15}N, would dilute possible radiogenic ^{40}Ar.

6. Discussion

6.1. Relationships among different fluids in the Mesozoic carbonate reservoir

As reported in previous studies, geothermal fields in central Italy produce Na-Cl type fluids with high NH_4 and B contents (Table 5). At Latera, geothermal fluids are produced from fractures in the carbonatic reservoir (Bertrami et al., 1984), whereas those at Mt. Amiata are mainly hosted in the Paleozoic metamorphic basement (Bertini et al., 1995). Salinity and chemical composition at both sites strongly dif-

fer from the mean chemical composition of the springs related to circulation in the same geological formations. As mentioned above, some of the thermal and cold springs (#33, #35, #36, #47), although located far from the discovered geothermal fields, have a Na-Cl composition which may suggest a leakage of the geothermal fluids in their circuits. Thermal spring #72 and a few of the nearby saline cold waters which locate near the coast, lie along the Cl/Br = 290 dilution line of unmodified seawater (Fig. 5). In contrast, thermal waters from the Siena basin fall along the line of Cl/Br = 750 suggesting a different deep saline endmember. Geothermal fluids from Mt. Amiata are along the line of Cl/Br = 500 and differ from those of Latera, since the latter have higher Cl/Br ratios (1000–2000). Setting aside the Latera geothermal samples that are scattered in the diagram, all the other groups have a parallel trend with respect to that of 'fresh' seawater in the Cl–Br diagram in Fig. 5. The excess of Cl with respect to the Cl/Br = 290 line can be explained as the result of HCl addition to the solutions after hydrolisis of Na-Cl (Fournier and Thompson, 1993) from brines located in deep portions of the crust characterized by extremely low permeability. Similar HCl enrichments have already been reported for the Larderello geothermal field (Truesdell et al., 1989; Duchi and Minissale, 1993), where residual magmatic brines

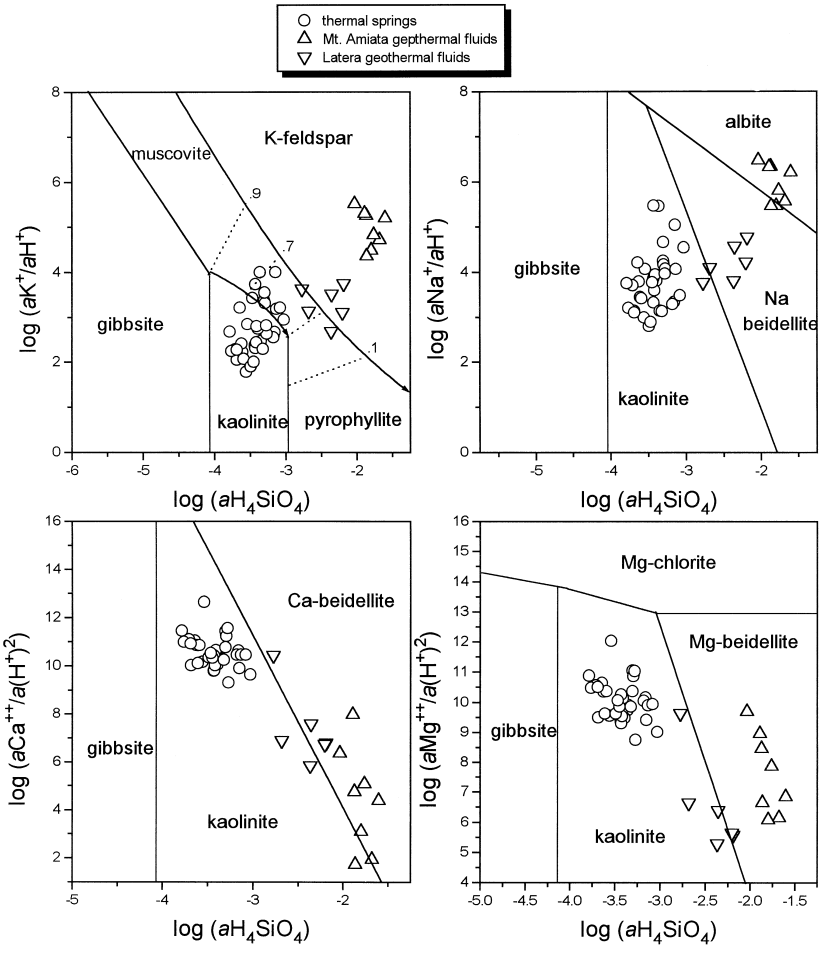

Fig. 13. Activity diagrams for K, Na, Ca, Mg vs. silica on both thermal spring samples and geothermal liquid phases (Nesbitt and Cramer, 1993).

have been suggested to be present under the vapor producing zone (D'Amore and Bolognesi, 1994). Thus, it seems reasonable to hypothesize the presence of residual magmatic brines with high Cl/Br ratio at Latera and Mt. Amiata, and possibly the Siena basin.

The majority of thermal springs are calcite-, aragonite-, dolomite- and quartz-saturated and all these minerals are well represented in veins in the Mesozoic limestone formations (Bertini et al., 1985; Cavarretta et al., 1985). Although these waters have mainly a Ca-SO_4 composition, none of them is anhydrite saturated. This is due to the CO_2 release at their exit, that causes precipitation of travertine substracting Ca ions from the solution resulting the undersaturation of gypsum or anhydrite.

Those thermal springs where $Al_{(tot)}$ is > 0.02 mg/kg (i.e. above the instrumental detection limit) are also saturated in several silicate minerals such as kaolinite, illite, smectite, etc. As these minerals are present at very low percentages in the Mesozoic limestone formations, both as primary and hydrothermal minerals, it is possible that they are derived from dissolution of argillitic alteration zones (< 150°C) overlying the reservoir (Cavarretta et al., 1985). In contrast, Gianelli and Scandiffio (1989) have calculated using the EQ3/6 software package (Wolery, 1979) that the geothermal fluids at Latera and the reservoir rock are in a thermodynamic equilibrium with primary feldspars. By plotting values in the activity diagram for the main cations (Na, K, Ca and Mg) vs. SiO_2 (Fig. 13), it is shown that the Mt. Amiata fluids fall effectively in the field of stability of primary minerals (feldspars), while the thermal springs fall in the stability field of kaolinite representing lower temperature supergenic conditions.

6.2. Geothermometry

Temperatures at the top of the carbonate reservoir are relatively well known in the study area (Fig. 14; C.N.R., 1982). Their distribution has been drawn using temperatures measured at the geothermal wells at Travale, Latera and Mt. Amiata and temperatures calculated from shallow holes drilled for thermal gradient prospections in areas where the carbonate top is known through geophysical surveys. In the reservoir outcropping areas temperatures are those of

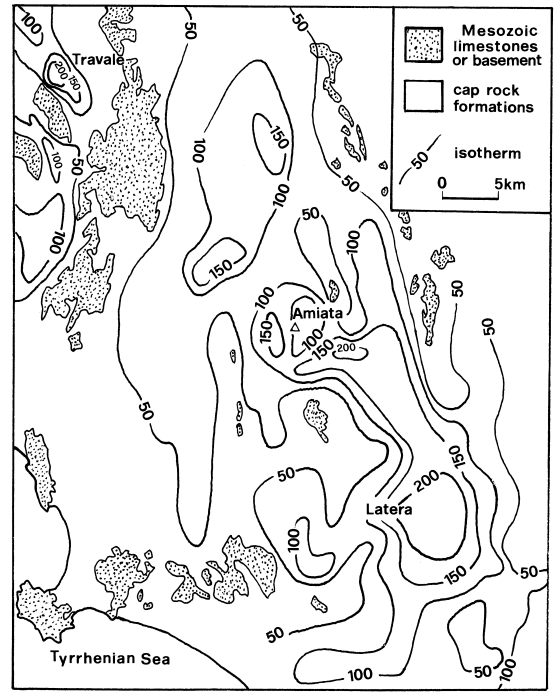

Fig. 14. Estimated temperatures (°C) at the top of the Mesozoic carbonate formations (same area as in Fig. 1; redrawn after C.N.R., 1982).

thermal springs (generally < 50°C), whereas in the remaining areas (mainly along the Tyrrhenian coast) they derive from the application of the silica geothermometer to the thermal springs discharging in the area (C.N.R., 1982). Such waters commonly discharge at a high flow rate, thus, it is likely that silica concentrations are not reset during ascent from the reservoir to the land surface and, hence, the silica-based geothermometers provide accurate indications of reservoir temperatures near the top of the carbonate aquifer.

By applying geothermometers to these springs and by considering the hydrogeochemical features of both spring waters, natural gases and geothermal fluids as described so far, some insights can be derived for temperature estimates at depth in those areas affected by the presence of the regional Ca-SO_4 aquifer. Results of geothermometric calculations are reported in Tab. 7. For most samples, two types of temperatures are calculated: (1) a low-temperature (< 100°C) calculated with the chalcedony (Fournier,

1973), quartz (Fournier and Rowe, 1966) and K^2/Mg (Giggenbach et al., 1983) geothermometers; and (2) higher temperature (ranging from 150 to 300°C) calculated with the Na/K, Na–K–Ca (Fournier and Truesdell, 1973) and Na/Li (Fouillac and Michard, 1981; Kharaka et al., 1982) geothermometers. Since thermal water discharge and recharge areas are very close, the springs might locate at the basal level of karstic circulation in a large unconfined aquifer characterized by a deep convective circuit in limestones (Minissale and Duchi, 1988), whose thickness in the area is potentially more than 3 km (Buonasorte et al., 1991). In spite of this, addition of Cl-rich brines to the Ca-SO_4 aquifer is plausible while it is highly likely in the Siena basin. By applying the geothermometric technique proposed by Giggenbach (1986) and reported in the Na–K–Mg ternary diagram in Fig. 15, additions of cations from such brines are partly responsible for the observed trend between the immature Mg corner and the equilibrium line, the latter being the result of the isochemical re-crystallization of a primary rock into a secondary mineral assemblage (Giggenbach, 1988). Although this is relatively clear for the Siena basin samples, most of the remaining thermal springs are close to the Mg corner, suggesting that their temperatures at depth are < 100°C.

Another estimation of deep reservoir temperatures can be obtained with geothermometers based on the gas composition. Although some gas components may partly solubilize in waters and suffer re-equilibration processes at low temperature, their less reactive components (H_2, CH_4, N_2) are likely to reflect their deep chemical equilibration temperature. Among the many diagrams proposed by Giggenbach (1991, 1993); Giggenbach and Soto, 1992; Giggenbach and Glover, 1992; Giggenbach et al., 1994), we focused our attention to the CH_4/CO_2 vs. CO/CO_2

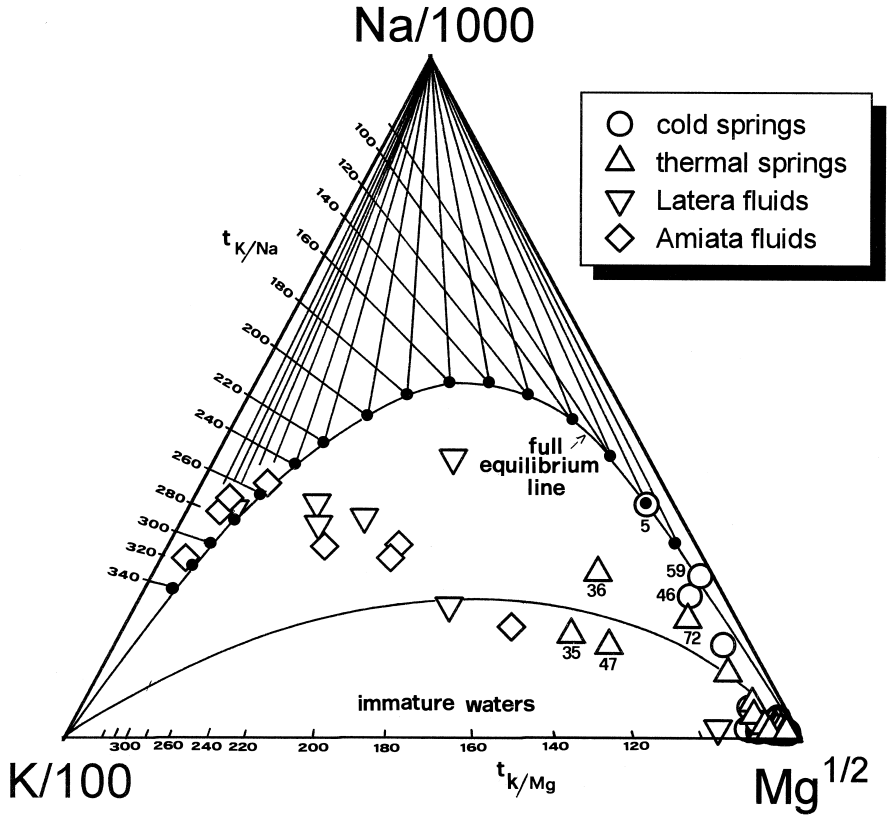

Fig. 15. $K/100–Na/1000–Mg^{1/2}$ ternary diagram (Giggenbach, 1988). See text.

diagram (Fig. 16). This diagram is based on the assumption that the gas phase, equilibrated either in vapor or liquid phases, is constrained by the FeO–$FeO_{1.5}$ pair, which is believed to be the main mineralogical buffer in a relatively wide interval of hydrothermal temperatures (Giggenbach, 1987). Similarly to Fig. 15, where geothermal waters from productive wells in the Mt. Amiata area were close to the full equilibrium line at bottom hole temperatures, geothermal gases in Fig. 16 are in the inner part of the liquid–vapour equilibrium boundaries (two phases) at temperatures comparable with those that occur in the reservoir (250–300°C). On the other hand, most of the natural gases associated with the springs (especially the N_2-rich 'thermal' samples), in spite of showing evidence of disequilibrium composition in Fig. 16, indicate high reservoir temperatures. If non referred to deep reservoirs below the carbonate reservoir inside the metamorphic basement (which is likely for those gases emerging at the boundary of limestones), these higher temperatures apply to the confined geothermal zones of the carbonate reservoir, from which the Cl-rich brines leak up into the Ca-SO_4 aquifer.

6.3. Geothermal gradients, hydrogeology and deep circulation

The distribution pattern of deep temperatures in central Italy (CEE, 1988) shows that, in response to an upper-mantle rising at 20–25 km depth (Calcagnile and Panza, 1979) with consequent higher thermal gradients, the isotherms tend to flatten in the upper part of the crust along the peri-tyrrhenian margin. The mean geothermal gradient is about 80–100°C/km leading to temperatures of 250–400°C at 3–4 km depth in those areas where the limestones are relatively thin and not affected by the circulation of meteoric waters. These deep temperatures agree well with those directly observed in the geothermal fields, even where the very shallow thermal gradient is as high as 500°C/km (Larderello, Cataldi et al., 1963). In contrast low gradients (up to 40°C/km) have been measured in those areas where thick Mesozoic limestone formations occur (e.g. Torre Alfina; Buonasorte et al., 1991). The lower gradients can be explained by different Moho depth, however, the contrast in the thickness of Mesozoic limestones

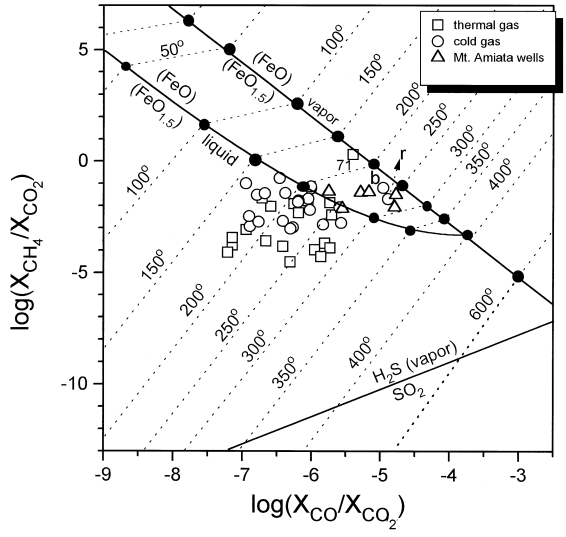

Fig. 16. Log(CH_4/CO_2) vs. log(CO/CO_2) diagram (Giggenbach, 1991). See text.

suggests that the permeability of the limestone is high and cold meteoric water circulation occur in the formation, causing a decrease in the geothermal gradient locally, and dilution of both the deep-seated waters and gases.

Confined thermal Cl-rich brines possibly leaking from the geothermal reservoirs may mix with the Ca-SO_4 waters while the associated gas components, especially the more soluble (CO_2, H_2S), may be absorbed in these waters in the carbonate aquifer. Other possible processes related to this mixing are:

(1) mobilization and re-deposition of sulphides (Tuscany Metallogenic Province, Tanelli, 1983);

(2) alteration of primary silicates and re-deposition in hydrothermal veins (Cavarretta et al., 1982, 1985);

(3) dissolution and/or deposition of anhydrite and/or calcite at the boundaries of the geothermal systems (Marini and Chiodini, 1994);

(4) modification of the water chemistry to HCO_3–SO_4 chemical compositions through the dissolution of CO_2 and H_2S which are likely components in geothermal fluids;

(5) changing the composition of gases associated to the springs, from CO_2-rich to N_2-rich, as a function of the meteoric water/deep fluid ratio.

Since these processes are enhanced in areas of large thermal gradients and large permeability, they

are most developed both at the top of the convective circuits at the boundaries of the low-permeability flysch formations and at the bottom of the convective cells which usually coincides with the base of the Mesozoic limestones. In the Paleozoic basement and the lateral margins of the carbonate outcrops close to the geothermal systems, the hydrologic and thermodynamic conditions may change dramatically over short distances, leading to self-sealed low pressure zones typically described for the Larderello–Travale geothermal fields (Facca and Tonani, 1967; Minissale, 1991b). These zones, generally not directly connected with the overlying unconfined aquifer(s), may be underlain by deeper high-enthalpy reservoirs in the Paleozoic metamorphic basement. Such deep reservoirs are found in both the Mt. Amiata (Bertini et al., 1995) and Travale (Barelli et al., 1995) fields, where fluids with different temperature are produced from the main carbonate reservoir at 200–250°C and the basement at temperature ranging from 300 to 350°C.

Geodynamic implications are suggested by the regional $^3He/^4He$ isotopic distribution in the gas manifestations (Fig. 12). Central Italy has generally been considered to be in an extensional phase, which would favor the intrusion of crustal and subcrustal magmas as in the Mt. Amiata and Mts. Vulsini volcanic areas (Conticelli and Peccerillo, 1992). However, recent tectonic interpretations of the post-orogenic structures imply that the Northern Apennines might be in a compressive phase, where basins are not the result of structures crossing the crust, but formed by folding and trusting in a compressive tectonic regime in shallow environment ('piggy-back ore pearced type basins'; Boccaletti et al., 1995). The $^3He/^4He$ isotopic ratios in the sampled gases reported as R/R_A areal distribution in Fig. 12 suggest significant gas contributions from the mantle only at Travale, which is not far from the already reported ^{3}He-anomaly area of the Larderello field (Hooker et al., 1985). In the remaining areas, especially in the Siena–Radicofani basin, the $^3He/^4He$ ratio is low, indicating little mantle contribution to the area and/or high production of radiogenic ^{4}He in the shallow crust, which is consistent with the recent hypothesis suggested by Boccaletti et al. (1995). Since the volcanic activity at Mt. Amiata and Mts. Vulsini is quite recent (< 0.2 Ma; Fornaseri, 1985), the occurrence of the described large thermal anomalies in the study area would have to be considered a residual phase of a regional mantle activity preceding the present compressive regime.

7. Summary and conclusions

The flow systems for both thermal and cold springs in a large sector of central Italy are fed by waters of meteoric origin. Although contributions into the carbonate reservoir of saline waters driven down from aquifers in the Neogene series and/or residual Cl-rich magmatic brines leaking from confined self-sealed geothermal systems are very likely in the Mt. Amiata, Siena basin and Latera, respectively, the regional aquifer maintains a general Ca-SO_4 character all over the area. This is due to the large convective circulation of meteoric-originated waters in high permeable limestones that buffers the input of fluids of different composition. The convective circulation in the limestone dramatically lowers the thermal gradient where the limestones are tectonically thickened as happens at Torre Alfina, where temperatures < 200°C are measured at 4.5 km depth (Buonasorte et al., 1991).

The behavior of the gas phase is, in some ways, similar to that of thermal waters. The huge amount of CO_2 produced and/or accumulated inside the confined geothermal fields in the carbonates and the basement rises and dissolves in the colder upper parts of the regional aquifer in those zones where it is unconfined. In those areas where the gas flow is higher, or the permeability of the carbonates is reduced (high gas/water ratio), the chemical composition of the gas phase may be only slightly modified by contamination of N_2 driven down in the reservoir by rainwater. By contrast, the higher the amount of the meteoric gas component involved near the recharge areas, the higher the N_2 content. As a consequence, the gas composition present at depth is not always the same as at the surface.

Reservoir temperature estimates based on geothermometric calculations for thermal springs and gases can be considered unreliable in the absence of drill hole measurements or knowledge of the process that affects the chemistry of the surficial features. The application of fast re-equilibrating geothermometers

(such as SiO_2) to the springs discharging in the Mt. Amiata, Latera and Travale areas would have not suggested the presence of the geothermal systems, but only revealed the convective circulation in the unconfined upper parts of the carbonate reservoir. Nevertheless, it can reasonably be hypothesized that the $\delta^{18}O$ shift observed in the two Na-Cl type thermal waters from the Siena basin (samples #35 and #47) and the high H_2 content in the gas sample from Selvena (sample #r) situated at about 10–15 km southwest of Mt. Amiata, derive from two thermally anomalous areas not yet discovered by drilling.

$^3He/^4He$ isotopic ratios from the 26 gas samples investigated (excluding Travale) suggest little contribution of ^3He from upper mantle. This is not consistent with the occurrence of the Neogene post-orogenic basins and the Quaternary primary undersaturated magmas at Mts. Vulsini, where large ^3He degassing from active mantle-related structures would be expected. Thus, the existing thermal anomalies in the Mt. Amiata–Vulsini region would have to be related to preceding Pliocene tensive phases.

Acknowledgements

Many thanks are due to ENEL (Italian Electric Agency) for giving us access to a large set of water and gas geochemical data. E. Corazza, M. Pennisi, S. Pieri, U. Rossi and M. Valenti have contributed to the sampling campaigns and the laboratory analyses. Special thanks to G. Scandiffio, A. Ceccarelli and A. Ridolfi (ENEL, Pisa, Italy) for their useful suggestions in the early draft versions of the manuscript.The text greatly improved in clarity after the critical review of M. Sorey and H. Shinohara, who are warmly thanked.

References

Abbate, E., Bortolotti, V., Passerini, P., Sagri, M., Sestini, G., 1970. Development of the northern Apennines geosyncline. Sediment. Geol. 4, 207–642.

Arnorsson, S., 1983. Chemical equilibria in Icelandic geothermal systems — implications for chemical geothermometry investigations. Geothermics 12, 119–128.

Baldi, P., Ferrara, G.C., Masselli, L., Pieretti, G., 1973. Hydrogeochemistry of the region between Mt. Amiata and Rome. Geothermics 2, 124–141.

Ball, J.W., Nordstrom, D.K., 1991. User's manual for WATEQ4F, with revised thermodynamic data base and test cases for calculating speciation of major, trace and redox elements in natural waters. U.S. Geol. Surv., Open-File Rep. 91-183, 1–189.

Barberi, F., Innocenti, F., Ricci, C.A., 1971. Il magmatismo nell' Appennino centro-settentrionale. Rend. Soc. Ital. Mineral. Petrol. 27, 169–213.

Barelli, A., Bertani, R., Cappetti, G., Ceccarelli, A., 1995. An update on Travale–Radicondoli geothermal field. Proc. World Geothermal Congress, Florence, Italy, 18–31 May 1995, pp. 1581–1586.

Barnes, I., Irwin, W., White, D., 1978. Global distribution of carbon dioxide and major zones of seismicity. U.S. Geol. Surv., Open-File Rep. 78-39.

Barnes, I., Irwin, W., White, D., 1984. Map showing distribution of CO_2 springs and major zones of seismicity. U.S. Geol. Surv., Misc. Invest. Ser., Map I-1528.

Batini, G., Bertini, G., Gianelli, G., Pandeli, E., Puxeddu, M., 1995. Deep structure age and evolution of the Larderello–Travale geothermal field. Geotherm. Resour. Counc. Trans. 9, 253–259.

Battaglia, A., Ceccarelli, A., Ridolfi, A., Frohlich, K., Panichi, C., 1992. Radium isotopes in geothermal fluids in central Italy. Proc. Int. Symp. on Isotope Techniques in Water Resources Development, I.A.E.A., 11–15 March 1991, Vienna, pp. 363–383.

Bencini, A., Duchi, V., 1986. Boron content of thermal waters of Tuscany and Latium (Italy). Proc. 5th Water–Rock Interaction Congress, Reykjavik, Iceland, 8–17 Aug. 1986, pp. 45–47.

Bencini, A., Duchi, V., Martini, M., 1977. Geochemistry of thermal springs of Tuscany. Chem. Geol. 19, 229–252.

Bertini, G., Gianelli, G., Pandeli, E., Puxeddu, M., 1985. Distribution of hydrothermal minerals in Larderello–Travale and Mt. Amiata geothermal fields (Italy). Geotherm. Resour. Counc. Trans. 9, 261–266.

Bertini, G., Cappetti, G., Dini, I., Lovari, F., 1995. Deep drilling results and updating of geothermal knowledge on the Monte Amiata area. Proc. World Geothermal Congress, Florence, Italy, 18–31 May 1995, pp. 1283–1286.

Bertrami, R., Cameli, G.M., Lovari, F., Rossi, U., 1984. Discovery of Latera geothermal field: problems of the exploration and research. Sem. on: Utilization of Geothermal Energy, Firenze, Italy, May 1984, pp. 1–18.

Bertrami, R., Cioni, R., Corazza, E., D'Amore, F., Marini, L., 1985. Carbon monoxide in geothermal gases; reservoir temperature calculations at Larderello (Italy). Geotherm. Resour. Counc. Trans. 9, 299–303.

Boccaletti, M., Bonini, M., Moratti, G., Sani, F., 1995. Nuove ipotesi sulla genesi e l'evoluzione dei bacini post-nappe in relazione alle fasi compressive Neogenico–Quaternarie dell'Appennino settentrionale. Scr. Doc. Acc. Naz. Sci. 14, 229–262.

Buonasorte, G., Cataldi, R., Ceccarelli, A., Costantini, A., D'Offizi, S., Lazzarotto, A., Ridolfi, A., Baldi, P., Barelli, A.,

Bertini, G., Bertrami, R., Calamai, A., Cameli, G.M., D'Aquino, C., Fiordelisi, A., Ghezzo, C., Lovari, F., 1988. Ricerca ed esplorazione nell'area geotermica di Torre Alfina (Lazio, Umbria). Boll. Soc. Geol. Ital. 107, 265–337.

Buonasorte, G., Pandeli, E., Fiordelisi, A., 1991. The Alfina 15 well: deep geological data from northern Latium (Torre Alfina geothermal area). Boll. Soc. Geol. Ital. 110, 823–831.

Calamai, A., Cataldi, R., Squarci, P., Taffi, L., 1970. Geology, geophysics and hydrogeology of the Mt. Amiata geothermal field. Geothermics Spec. Iss. 1, 1–9.

Calamai, A., Cataldi, R., Locardi, E., Praturlon, A., 1976a. Distribuzione delle anomalie geotermiche nella fascia preappenninica Tosco–Laziale (Italia). Proc. Symp. Int. sobre Energia Geotermica en America Latina, Guatemala City, 18–23 Oct., pp. 189–229.

Calamai, A., Cataldi, R., Dall'Aglio, M., Ferrara, G.C., 1976b. Preliminary report on the Cesano hot brine deposit (northern Latium, Italy). Proc. 2nd U.N. Symp. on the Development and Use of Geothermal Energy, San Francisco, CA, 20–29 May 1975, 305–313.

Calcagnile, C., Panza, C.F., 1979. Crustal and upper mantle structures beneath the Apennines region as inferred from the study of Reyleigh waves. J. Geophys. 45, 319–327.

Calore, C., Celati, R., Gianelli, G., Norton, D., Squarci, P., 1981. Studi sull'origine del sistema geotermico di Larderello. In: Proc. 2° Semin. Inform. su 'Energia Geotermica: prospettive aperte dalle ricerche del CNR'. CNR PFE SI-2, Rome, pp. 218–225.

Carella, R., Verdiani, A., Palmerini, C., Stefani, G.C., 1985. Geothermal activity in Italy: present status and future prospects. Geothermics 14, 247–254.

Cataldi, R., Rendina, M., 1973. Recent discovery of a new geothermal field: Alfina. Geothermics 2, 106–116.

Cataldi, R., Stefani, G.C., Tongiorgi, E., 1963. Geology of Larderello region (Tuscany): contribution to the study of the geothermal basin. In: Nuclear Geology on Geothermal Areas, Spoleto, Italy, pp. 235–265.

Cavarretta, G., Gianelli, G., Puxeddu, M., 1982. Formation of authigenic minerals and their use as indicators of the physicochemical parameters of the fluid in the Larderello–Travale geothermal field. Econ. Geol. 77, 1071–1084.

Cavarretta, G., Gianelli, G., Scandiffio, G., Tecce, F., 1985. Evolution of the Latera geothermal system II: metamorphic, hydrothermal mineral assemblages and fluid chemistry. J. Volcanol. Geotherm. Res. 26, 337–364.

Ceccarelli, A., Celati, R., Grassi, S., Minissale, A., Ridolfi, A., 1987a. The southern boundary area of the Larderello geothermal field. Geothermics 16, 505–516.

Ceccarelli, A., Corazza, E., Magro, G., Pieri, S., Rossi, U., 1987b. Prospezione di alcuni gas del suolo nei Monti Vulsini. ENEL (Italian National Electricity Agency), Pisa, Intern. File Rep., pp. 1–40.

Ceccarelli, A., Ridolfi, A., Pieri, S., Corazza, E., Magro, G., Scandiffio, G., Valenti, M., 1988. Prospezione idrogeochimica 'Amiata nord'. ENEL (Italian National Electricity Agency), Pisa, Italy, Intern. File Rep., pp. 1–65.

Ceccarelli, A., Perticone, I., Ridolfi, A., Scandiffio, G., Valenti, M., Corazza, E., Magro, G., 1989. Prospezione idrogeochimica 'Roccastrada'. ENEL (Italian National Electricity Agency), Pisa, Intern. File Rep., pp. 1–64.

Ceccarelli, A., Perticone, I., Ridolfi, A., Scandiffio, G., Corazza, E., Magro, G., Pennisi, M., 1991. Prospezione idrogeologica e geochimica dell'area denominata Roccalbegna ('Amiata SW'). ENEL (Italian National Electricity Agency), Pisa, Intern. File Rep., pp. 1–86.

CEE, 1988. In: Haenel, R., Staroste, E. (Ed.), Atlas of Geothermal Resources in the European Community. Schaefer, Hannover.

Celati, R., Grassi, S., D'Amore, F., Marcolini, L., 1991. The low temperature hydrothermal system of Campiglia, Tuscany (Italy): a geochemical approach. Geothermics 20, 67–81.

Chiodini, G., Giaquinto, S., Frondini, F., Santucci, A., 1991. Hydrogeochemistry and hydrogeology of the Canino hydrothermal system (Italy). Geothermics 20, 329–342.

C.N.R., 1982. Contributo alla conoscenza delle potenzialita' geotermiche della Toscana e del Lazio. C.N.R. PFE RF-15, Rome.

Conticelli, S., Peccerillo, A., 1992. Petrology and geochemistry of potassic and ultrapotassic volcanism in central Italy: petrogenesis and inferences on the evolution of the mantle source. Lithos 28, 221–240.

Craig, H., 1963. Isotopic variations in meteoric waters. Science 123, 1702–1703.

D'Amore, F., Bolognesi, L., 1994. Isotopic evidence for a magmatic contribution to the fluids of the geothermal systems of Larderello and The Geysers, California. Geothermics 23, 21–32.

D'Amore, F., Panichi, C., 1980. Evaluation of deep temperatures of hydrothermal systems by a new gas geothermometer. Geochim. Cosmochim. Acta 44, 549–556.

D'Amore, F., Panichi, C., Squarci, P., Bertrami, R., Ceccarelli, A., 1979. Studio idrogeologico e geochimico dei sistemi termali della zona di Latera–Canino (Lazio settentrionale). In: Proc. 1° Semin. Inform. on 'Energia Geotermica: prospettive aperte dalle ricerche del CNR', CNR PFE SI-1, Rome, pp. 470–481.

Drever, J.I., 1982. The Geochemistry of Natural Waters. Prentice-Hall, Englewood Cliffs, NJ, pp. 82–85.

Duchi, V., Minissale, A., 1993. A new hypothesis on the production of Cl-bearing steam in the Larderello geothermal field, Italy. Chem. Erde 53, 259–271.

Duchi, V., Minissale, A., 1995. Distribuzione delle manifestazioni gassose nel settore peritirrenico tosco-laziale e loro interazione con gli acquiferi superficiali. Boll. Soc. Geol. Ital. 114, 337–351.

Duchi, V., Minissale, A., Romani, L., 1985. Studio geochimico su acque e gas dell'area geotermica Lago di Vico–M.ti Cimini (Viterbo). Atti Soc. Tosc. Sci. Nat. 92, 237–254.

Duchi, V., Minissale, A., Prati, F., 1987a. Chemical composition of thermal springs, cold springs, streams, and gas vents in the Mt. Amiata geothermal region (Tuscany, Italy). J. Volcanol. Geotherm. Res. 31, 321–332.

Duchi, V., Minissale, A., Ortino, S., Romani, L., 1987b. Geother-

mal prospecting by geochemical methods on natural gas and water discharges in the Vulsini Mts volcanic district (central Italy). Geothermics 16, 147–157.

Duchi, V., Minissale, A., Paolieri, M., Prati, F., Valori, A., 1992. Chemical relationship between discharging fluids in the Siena–Radicofani graben and the deep fluids produced by the geotheermal fields of Mt. Amiata, Torre Alfina, and Latera (central Italy). Geothermics 21, 401–413.

Ellis, A.J., 1971. Magnesium ion concentrations in the presence of Mg-chlorite, calcite, carbon dioxide, and quartz. Am. J. Sci. 271, 481–489.

Facca, G., Tonani, F., 1967. The self-sealing geothermal field. Bull. Volcanol. 30, 271–273.

Fancelli, R., Nuti, S., 1975. Studio sulle acque termali e minerali del graben di Siena. Boll. Soc. Geol. Ital. 94, 135–155.

Faure, G., 1986. Principles of Isotope Geology. Wiley, New York, NY, 589 pp.

Ferrari, L., Conticelli, S., Burlamacchi, L., Manetti, P., 1996. New geologic and volcanological data on the Mt. Amiata silicic complex. Acta Vulcanol. 8, 41–56.

Fornaseri, M., 1985. Geochronology of volcanic rocks from Latium (Italy). Rend. Soc. Ital. Mineral. Petrol. 40, 73–105.

Fouillac, C., Michard, G., 1981. Sodium/lithium ratios in water applied to geothermometry of geothermal reservoirs. Geothermics 10, 55–70.

Fournier, R.O., 1973. Silica in thermal waters:Laboratory and field investigations. Proc. Int. Symp. on Hydrogeochem. Biogeochem., Tokyo, pp. 122–139.

Fournier, R.O., 1979. A revised equation for the Na/K geothermometer. Geotherm. Resour. Counc. Trans. 3, 221–224.

Fournier, R.O., Rowe, J.J., 1966. Estimation of underground temperatures from the silica content of water from hot springs and wet-steam wells. Am. J. Sci. 264, 685–697.

Fournier, R.O., Thompson, J.M., 1993. Composition of steam in the system NaCl–KCl–H_2O–quartz at 600°C. Geochim. Cosmochim. Acta 57, 4365–4375.

Fournier, R.O., Truesdell, A.H., 1973. An empirical Na–K–Ca geothermometer for natural waters. Geochim. Cosmochim. Acta 37, 515–525.

Francalanci, G., 1959. Contributo per la conoscenza delle manifestazioni termali della Toscana. Atti Soc. Tosc. Sci. Nat. 65, 372–432.

Gatt, J.R., Carmi, I., 1970. Evolution of the isotopic composition of atmospheric waters in the Mediterranean Sea area. J. Geophys. Res. 75, 3032–3048.

Gianelli, G., 1985. On the origin of Geothermal CO_2 by metamorphic processes. Boll. Soc. Geol. Ital. 104, 575–584.

Gianelli, G., Scandiffio, G., 1989. The Latera geothermal system (Italy): chemical composition of the geothermal fluid and hypotheses on its origin. Geothermics 18, 447–463.

Gianelli, G., Puxeddu, M., Batini, F., Bertini, G., Dini, I., Pandeli, E., Nicolich, R., 1988. Geological model of a young volcano-plutonic system: the geothermal region of Monte Amiata (Tuscany, Italy). Geothermics 17, 719–734.

Giggenbach, W.F., 1975. A simple method for the collection and analysis of volcanic gas samples. Bull. Volcanol. 39, 132–145.

Giggenbach, W.F., 1980. Geothermal gas equilibria. Geochim. Cosmochim. Acta 44, 2021–2032.

Giggenbach, W.F., 1986. Graphycal techniques for the evaluation of water–rock interaction conditions by use of Na, K, Mg and Ca contents of discharge waters. Proc. 8th New Zealand Geothermal Workshop, pp. 37–44.

Giggenbach, W.F., 1987. Redox processes governing the chemistry of fumarolic gas discharges from White Island, New Zealand. Appl. Geochem. 2, 143–161.

Giggenbach, W.F., 1988. Geothermal solute equilibria; derivation of Na–K–Mg–Ca geoindicators. Geochim. Cosmochim. Acta 52, 2749–2765.

Giggenbach, W.F., 1991. Chemical techniques in geothermal exploration. In: D'Amore, F. (Ed.), Application of Geochemistry in Geothermal Reservoir Development. UNITAR, Rome, pp. 119–144.

Giggenbach, W.F., 1993. Redox control of gas compositions in the Philippine volcanic-hydrothermal systems. Geothermics 22, 575–587.

Giggenbach, W.F., Glover, R.B., 1992. Tectonic regime and major processes governing the chemistry of water and gas discharges from the Rotorua geothermal field, New Zealand. Geothermics 21, 121–140.

Giggenbach, W.F., Soto, R.C., 1992. Isotopic and chemical composition of water and steam discharges from volcanic–magmatic–hydrothermal systems of the Guanacaste geothermal province, Costa Rica. Appl. Geochem. 7, 309–332.

Giggenbach, W.F., Gonfiantini, R., Jangi, B.L., Truesdell, A.H., 1983. Isotopic and chemical composition of Parbaty Valley geothermal discharges, NW-Himalaya. Geothermics 12, 199–222.

Giggenbach, W.F., Sano, Y., Wakita, H., 1993. Isotopic composition of helium, and CO_2 and CH_4 contents in gases produced along the New Zealand part of a convergent plate boundary. Geochim. Cosmochim. Acta 57, 3427–3455.

Giggenbach, W.F., Sheppard, D.S., Robinson, B.W., Stewart, M.K., Lyon, G.L., 1994. Geochemical structure and position of the Waiotapu geothermal field, New Zealand. Geothermics 23, 599–644.

Giraud, A., Dupuy, C., Dostal, J., 1986. Behaviour of trace elements during the magmatic processes in the crust: application to acidic volcanic rocks of Tuscany (Italy). Chem. Geol. 57, 269–288.

Honma, H., Itihara, Y., 1981. Distribution of ammonium in minerals of metamorphic and granitic rocks. Geochim. Cosmochim. Acta 45, 983–988.

Hooker, P.J., Bertrami, R., Lombardi, S., O'Nions, R.K., Oxburgh, E.R., 1985. Helium-3 anomalies and crust–mantle interaction in Italy. Geochim. Cosmochim. Acta 49, 2505–2513.

Jenden, P.D., Kaplan, I.R., Poreda, R.J., Craig, H., 1988. Origin of nitrogen-rich natural gases in the California Great Valley: evidence from helium, carbon and nitrogen isotope ratios. Geochim. Cosmochim. Acta 52, 851–861.

Kissin, I.G., Pakhomov, S.I., 1967. The possibility of carbon dioxide generation at depth at moderately low temperature. Dokl. Akad. Nauk SSSR 174, 451–454.

Kharaka, Y.K., Lico, M.S., Law, L.M., 1982. Chemical geotermometers and their application to formation waters from sedimentary basins. In: Thermal History of Sedimentary Basins. Springer, New York, NY, pp. 99–117.

Kyser, T.K., 1986. Stable isotope variations in the mantle. In: Valley, J.M., Taylor, Jr., H.P., O'Neil, J.R. (Eds.), Stable Isotopes in High Temperature Geological Processes. Rev. Mineral. 16, 141–164.

Langelier, W., Ludwig, H., 1942. Graphical methods for indicating the mineral character of natural waters. J. Am. Water Assoc. 34, 335–352.

Lotti, B., 1910. Geologia della Toscana. Mem. Descr. Carta Geol. d'Italia, Tipog. Naz., Rome, pp. 1–484.

Marini, L., Chiodini, G., 1994. The role of carbon dioxide in the carbonate–evaporite geothermal systems of Tuscany and Latium (Italy). Acta Volcanol. 5, 95–104.

Marini, L., Chiodini, G., Cioni, R., 1986. New geothermometers for carbonate-evaporite geothermal reservoirs. Geothermics 15, 77–86.

Marty, B., O'Nions, R.K., Oxburg, E.R., Martel, D., Lombardi, S., 1992. Helium isotopes in Alpine regions. Tectonophysics 206, 71–78.

Minissale, A., 1991a. Thermal springs in Italy: their relation to recent tectonics. Appl. Geochem. 6, 201–212.

Minissale, A., 1991b. The Larderello geothermal field: a review. Earth Sci. Rev. 31, 133–151.

Minissale, A., Duchi, V., 1988. Geothermometry on fluids circulating in a carbonate reservoir in north-central Italy. J. Volcanol. Geotherm. Res. 35, 237–252.

Minissale, A., Evans, W., Magro, G., Duchi, V., Vaselli, O., 1995. Gas manifestations in central Italy. Proc. World Geothermal Congress, Florence, 18–31 May 1995, pp. 1013–1017.

Minissale, A., Evans, W., Magro, G., Vaselli, O., 1997. Multiple source components in gas manifestations from north-central Italy. Chem. Geol. (in press).

Nesbitt, H.W., Cramer, J.J., 1993. Genesis and evolution of HCO3-rich grounwaters of Quaternary sediments, Pinawa, Canada. Geochim. Cosmochim. Acta 57, 4933–4946.

Nieva, D., Nieva, R., 1987. Developments in geothermal energy in Mexico, part 12; a cationic composition geothermometer for prospection of geothermal resources. Heat Recovery Syst. CHP 7, 243–258.

Pandeli, E., Castellucci, P., Bertini, G., 1991. The tectonic wedges complex of the Larderello area (southern Tuscany, Italy). Boll. Soc. Geol. Ital. 110, 621–629.

Panichi, C., 1982. Aspetti geochimici delle acque termali. In: Il graben di Siena. CNR PFE RF-9, Rome, pp. 61–72.

Panichi, C., Tongiorgi, E., 1976. Carbon isotopic composition of CO_2 from springs, fumaroles, mofettes, and travertines of central and southern Italy: a preliminary prospection method of geothermal areas. Proc. 2nd U.N. Symp. on the Development and Use of Geothermal Energy, San Francisco, CA, 20–29 May 1975, pp. 815–825.

Panichi, C., Celati, R., Noto, P., Squarci, P., Taffi, L., 1974. Oxygen and hydrogen isotope studies of the Larderello (Italy) geothermal field. In: Isotope Techniques in Groundwater Hydrology. IAEA–SM 2, 3–28.

Peccerillo, A., Manetti, P., Conticelli, S., 1987. Petrological characteristics and the genesis of the recent magmatism of south Tuscany and north Latium. Per. Mineral. 56, 167–183.

Poli, G., Frey, F.A., Ferrara, G., 1984. Geochemical characteristics of the south Tuscany (Italy) volcanic province: constraints on lava petrogenesis. Chem. Geol. 43, 203–221.

Puxeddu, M., 1984. Structure and late Cenozoic evolution of the upper lithosphere in southwest Tuscany (Italy). Tectonophysics 101, 357–382.

Sestini, F., 1932. Il mare pliocenico della Toscana meridionale. Mem. Geol. Geogr. G. Dainelli 2.

Tanelli, G., 1983. Mineralizzazioni metallifere e minerogenesi della Toscana. Mem. Soc. Geol. Ital. 25, 91–109.

Tonani, F., 1957. Il contenuto di fluoro e di boro in acque termominerali toscane. Atti Soc. Tosc. Sci. Nat. 64, 184–205.

Tonani, F., 1973. Equilibria that control the hydrogen content of geothermal gases. Phillips Pet. Co. Rep. (unpubl.).

Tonani, F., 1980. Some remarks on the application of geochemical techniques in exploration. In: Proc. Advances Europ. Geothermal Resources, Strasbourg, pp. 428–443.

Trevisan, L., 1951. Una nuova ipotesi sull'origine della termalita' di alcune sorgenti della Toscana. Ind. Miner. 2, 41–42.

Truesdell, A.H., 1976. Geochemical techniques in exploration. Proc. 2nd U.N. Symp. on the Development and Use of Geothermal Energy, San Francisco, CA, 20–29 May 1975, pp. 53–89.

Truesdell, A.H., Haizlip, J.R., Armannsson, H., D'Amore, F., 1989. Origin and transport of chloride in superheated geothermal steam. Geothermics 18, 295–304.

Vighi, L., 1958. Sulla serie triassica 'Cavernoso–Verrucano' presso Capalbio (Orbetello–Toscana) e sulla brecciatura tettonica delle serie evaporitiche, rocce madri del Cavernoso. Boll. Soc. Geol. Ital. 77, 221–235.

Vighi, L., 1966. Descrizione di alcuni sondaggi che hanno attraversato lenti anidritico-dolomitiche intercalate alle filladi triassiche (Verrucano) dei dintorni di Massa M.ma (Grosseto, Toscana). Atti Soc. Tosc. Sci. Nat. 72, 72–95.

Villa, I., Gianelli, G., Puxeddu, M., Bertini, G., Pandeli, E., 1987. Granitic dikes of 3.8 Ma age from a 3.5 km deep geothermal well at Larderello. Atti del Convegno di Verbania Univ. of Milan, Italy (abstract).

Wolery, T.J., 1979. Calculation of chemical equilibrium between acqueous solutions and minerals: the EQ3/6 software package. Lawrence Livermore Lab., Rep. UCRL-52658, pp. 1–41.